

1  
2  
3  
4  
5  
6  
7  
8  
9  
10  
11  
12  
13  
14  
15  
16  
17  
18  
19  
20  
21  
22  
23  
24

**Immunomodulators Targeting MARCO Expression Improve Resistance to Post-influenza  
Bacterial Pneumonia**

**Authors:** Muzo Wu<sup>1</sup>, John G. Gibbons<sup>2</sup>, Glen M. DeLoid<sup>1</sup>, Alice S. Bedugnis<sup>1</sup>, Rajesh K. Thimmulappa<sup>3</sup>, Shyam Biswal<sup>3</sup>, Lester Kobzik<sup>1,\*</sup>

**Affiliations:**

<sup>1</sup>Department of Environmental Health, Harvard School of Public Health, Harvard University, Boston, MA 02115, USA.

<sup>2</sup>Biology Department, Clark University, Worcester, MA 01610, USA.

<sup>3</sup>Department of Environmental Health Sciences, Bloomberg School of Public Health, Johns Hopkins University, Baltimore, MD 21205, USA.

Correspondence:  
Lester Kobzik, M.D.  
Dept. of Environmental Health  
Harvard T.H. Chan School of Public Health  
665 Huntington Ave.  
Boston, MA 02115  
[lkobzik@hsph.harvard.edu](mailto:lkobzik@hsph.harvard.edu)

25 **Abstract:**

26 Down-regulation of the alveolar macrophage (AM) macrophage receptor with collagenous  
27 structure (MARCO) leads to susceptibility to post-influenza bacterial pneumonia, a major cause  
28 of morbidity and mortality. We sought to determine whether immunomodulation of MARCO  
29 could improve host defense and resistance to secondary bacterial pneumonia. RNAseq analysis  
30 identified a striking increase of MARCO expression between days 9 and 11 after influenza  
31 infection and indicated important roles for Akt and Nrf2 in MARCO recovery. In vitro, primary  
32 human AM-like monocyte-derived macrophages (AM-MDMs) and THP-1 macrophages were  
33 treated with IFN $\gamma$  to model influenza effects. Activators of Nrf2 (sulforaphane) or Akt (SC79)  
34 caused increased MARCO expression and a MARCO-dependent improvement in phagocytosis  
35 in IFN $\gamma$ -treated cells, and improved survival in mice with post-influenza pneumococcal  
36 pneumonia. Transcription factor analysis also indicated a role for transcription factor E-box  
37 (TFEB) in MARCO recovery. Overexpression of TFEB in THP-1 cells led to marked increases  
38 in MARCO. The ability of Akt activation to increase MARCO expression in IFN $\gamma$ -treated AM-  
39 MDMs was abrogated in TFEB-knockdown cells, indicating Akt increases MARCO expression  
40 through TFEB. Increasing MARCO expression by targeting Nrf2 signaling or Akt-TFEB-  
41 MARCO pathway are promising strategies to improve bacterial clearance and survival in post-  
42 influenza bacterial pneumonia.

43

44 **Keywords:** Influenza; bacterial pneumonia; immunomodulators; macrophage receptor with  
45 collagenous structure (MARCO); interferon- $\gamma$  (IFN- $\gamma$ ); Nrf2; Akt; TFEB

46

47 **Introduction**

48 Secondary bacterial pneumonia contributes to the high mortality from seasonal and pandemic  
49 influenza (80) (23). The most common pathogens identified include *Streptococcus pneumoniae*,  
50 *Staphylococcus aureus*, and *Haemophilus influenzae*. Susceptibility to superimposed bacterial  
51 infection is highest approximately four to fourteen days after influenza onset (60). Multiple  
52 mechanisms underlie increased susceptibility (8, 15, 19, 22, 27, 33, 38, 41, 43-45, 49, 50, 65, 66,  
53 73, 79, 81, 82, 85, 91), including influenza virus-induced interferon- $\gamma$  (IFN $\gamma$ ), which reduces  
54 expression of the phagocytic receptor macrophage receptor with collagenous structure  
55 (MARCO) on alveolar macrophages (AMs) (73).

56 MARCO is a highly-conserved trimeric class A scavenger receptor (7) that mediates  
57 phagocytosis of unopsonized particles and bacteria, thereby playing a key role in innate host  
58 defense (5). Upregulation of MARCO expression enhances bacterial binding and phagocytosis,  
59 and alters cytokine expression (51). Dysregulation of MARCO expression leads to impaired  
60 phagocytosis and bacterial clearance, as illustrated by increased lung injury and inflammation in  
61 MARCO<sup>-/-</sup> mice exposed to pathogens or particulates (5, 11, 76). We might anticipate, therefore,  
62 that immunomodulators upregulating MARCO expression would improve innate immune  
63 function and enhance bacterial clearance in post-influenza bacterial pneumonia. Hence, we  
64 analyzed the dynamics of MARCO expression after influenza infection to identify novel  
65 immunomodulatory strategies. A striking recovery and increase in MARCO was observed  
66 between days 9 and 11 after influenza infection. RNAseq transcriptome profiling of AMs on  
67 these days showed that TFEB and Nrf2 were among the most over-represented transcription  
68 factors regulating differentially expressed genes during the recovery period of post-influenza  
69 MARCO expression.

70 Sulforaphane (SFN), an isothiocyanate present in cruciferous vegetables, increases  
71 macrophage MARCO expression and antibacterial function through Nrf2 signaling (25, 77). We  
72 investigated the effects of SFN on post-influenza host defenses. Treatment with SFN increased  
73 MARCO expression and phagocytosis in IFN $\gamma$ -treated AM-MDMs, and significantly improved  
74 bacterial clearance and survival in a mouse model of secondary pneumococcal pneumonia.

75 TFEB is an evolutionally conserved master gene of lysosomal biogenesis, autophagy, and  
76 lysosomal exocytosis (46, 61, 63), and plays an important role in regulating host defenses against  
77 pathogens (83) and responses to nutritional stress (64). Transcriptome profiling suggested  
78 important roles for Akt and the transcription factor EB (TFEB) in recovery of MARCO  
79 expression. Treatment with the Akt activator SC79 improved MARCO expression and bacterial  
80 phagocytosis in IFN $\gamma$ -treated AM-MDMs. However, the effects of Akt-induced MARCO  
81 expression in IFN $\gamma$ -treated AM-MDMs were blocked after TFEB knockdown with siRNAs. Akt  
82 activation also improved survival of mice with secondary bacterial pneumonia. These  
83 observations identify a novel role for TFEB in the post-influenza host response, as a mediator of  
84 Akt activation-induced MARCO upregulation.

85 Our data identify novel regulators of AM MARCO expression after influenza, and  
86 broaden the range of potential immunomodulatory strategies to improve host resistance to post-  
87 influenza secondary pneumonia.

88

89 **Methods**

90 *Cells*

91 Human alveolar macrophage (AM)-like monocyte-derived macrophages (AM-MDMs) were  
92 prepared as previously described (13, 71). Briefly, human monocytes (New York Biologics,  
93 Southampton, NY) were isolated from discarded normal blood by negative selection using  
94 RosetteSep (Stemcell Technologies, Vancouver, BC, Canada) and matured into AM-like  
95 macrophages (1, 88) by 10-11 days of culture in the Roswell Park Memorial Institute – 1640  
96 (RPMI-1640) medium containing 2 mM L-glutamine, 20 mM HEPES, 1 mM sodium pyruvate,  
97 4500 mg/L glucose, 10% fetal bovine serum, 100 IU/ml penicillin, 100 µg/ml streptomycin, and  
98 20 ng/ml human granulocyte/macrophage colony-stimulating factor (GM-CSF, Peprotech, Rocky  
99 Hill, NJ, USA). B6 cells are an immortalized cell line derived from alveolar macrophages  
100 obtained from normal C57Bl6 mice as detailed in the previous report (89).

101 Human monocyte cell line, THP-1 cells (ATCC TIB-202<sup>TM</sup>, Rockville, MD), were grown in  
102 RPMI-1640 medium containing 2 mM L-glutamine, 20 mM HEPES, 1 mM sodium pyruvate,  
103 4500 mg/L glucose, 1500 mg/L sodium bicarbonate, 10% fetal bovine serum, and 1% of  
104 penicillin-streptomycin. THP-1 cells were differentiated into macrophages by growing in media  
105 containing 100 nM phorbol 12-myristate 13-acetate (PMA) (Sigma Aldrich Co. LLC.) and 20  
106 ng/ml GM-CSF for 24 hours.

107 *Bacteria*

108 Green fluorescent protein (GFP) – expressing *Staphylococcus aureus* strain RN6390 was  
109 prepared as previously described (13). *Streptococcus pneumoniae* serotype 3 (strain

110 ATCC6303<sup>TM</sup>, Rockville, MD) was cultured on 5% sheep blood-supplemented agar plates  
111 (VWR International, Radnor, PA). Bacteria were grown overnight and resuspended in sterile  
112 phosphate buffered saline (PBS) prior to infection. Concentration of the bacterial suspension was  
113 determined by measuring the optical density at A<sub>600</sub> with a spectrophotometer and by colony  
114 forming units (CFUs).

### 115 ***Immunomodulator Assays***

116 AM-MDMs were prepared from primary human monocytes as previously described (13, 71).  
117 AM-MDMs or THP-1 cells were treated with human IFN $\gamma$  (10, 20, or 50 IU/ml, Peprotech,  
118 Rocky Hill, NJ, USA) for 20 to 24 hours to simulate effects of influenza infection, and  
119 simultaneously incubated with or without R,S-sulforaphane (5 or 10  $\mu$ M, LKT Laboratories, Inc.,  
120 St. Paul, MN, USA) or with or without SC79 (2, 5 or 8  $\mu$ g/ml, EMD Millipore, Billerica, MA,  
121 USA) before quantitation of MARCO expression or challenge with GFP-expressing *S. aureus*  
122 strain RN6390.

123 For the *in vivo* study of immunomodulator effects in post-influenza bacterial pneumonia, wild-  
124 type C57BL/6 male mice were treated intraperitoneally with sulforaphane (20 to 25 mg/kg per  
125 mouse), or subcutaneously with SC79 (20 mg/kg per day) on days 6 to 9 or 10 after influenza  
126 infection.

127 For the *in vitro* study of the EGCG effect in post-influenza bacterial pneumonia, AM-MDMs or  
128 THP1 cells were treated with human IFN $\gamma$  (10, 20, or 50 IU/ml, Peprotech, Rocky Hill, NJ,  
129 USA) for 20 to 24 hours to simulate influenza infection, and simultaneously incubated with or  
130 without EGCG (10 or 50 $\mu$ M, Sigma Aldrich Co. LLC.) before quantitation of MARCO  
131 expression or challenge with GFP-expressing *S. aureus* strain RN6390 by scanning cytometry.

132 ***Bronchoalveolar lavage (BAL)***

133 After euthanasia, the mouse trachea was cannulated with a 20-gauge catheter for bronchoalveolar  
134 lavage. For colony-forming unit studies, bronchoalveolar lavage was performed on day 2 after *S.*  
135 *pneumoniae* infection. Mouse lungs were lavaged with a total of 4 ml of PBS. Serial dilutions of  
136 the lavage fluid were spread on blood agar plates and incubated for 17 h at 37 °C before CFU  
137 counting. For cytokine/chemokine studies and collection of alveolar macrophages, mouse lungs  
138 were first lavaged with 0.5ml PBS via cannulation, followed by 5 lavages with 0.7 ml PBS. The  
139 first 1.2 ml of the total 4ml lavage fluid was centrifuged at 200g for 10 minutes at 4°C.  
140 Supernatants from BALF collected on days 3, 5, 7, 9, and 11 after influenza infection were used  
141 for cytokine/ chemokine analysis. Cell pellets were resuspended with the cells in the remaining  
142 2.8 ml lavage for each sample.

143 ***Cytokine analysis***

144 Cytokines/ chemokines in mouse BALF after influenza virus strain PR8 infection were measured  
145 by using Mouse Cytokine Array/ Chemokine Array 32-plex Panel (Eve Technologies, Calgary,  
146 Alberta, Canada). The 32 cytokines/ chemokines include eotaxin, granulocyte colony-stimulating  
147 factor (G-CSF), granulocyte macrophage colony-stimulating factor (GM-CSF), IFN $\gamma$ , IL-1 $\alpha$ , IL-  
148 1 $\beta$ , IL-2, IL-3, IL-4, IL-5, IL-6, IL-7, IL-9, IL-10, IL-12 (p40), IL-12 (p70), IL-13, IL-15, IL-  
149 17A, interferon gamma-induced protein (IP-10), ketatinocyte chemoattractant (KC), leukemia  
150 inhibitory factor (LIF), lipopolysaccharide-induced CXC chemokine (LIX), monocyte  
151 chemotactic protein 1 (MCP-1), macrophage colony-stimulating factor (M-CSF), monokine  
152 induced by gamma interferon (76), macrophage inflammatory protein 1- $\alpha$  (MIP-1 $\alpha$ ), macrophage  
153 inflammatory protein 1-  $\beta$  (MIP-1 $\beta$ ), macrophage inflammatory protein 2 (MIP-2), regulated on

154 activation, normal T cell expressed and secreted (RANTES), tumor necrosis factor  $\alpha$  (TNF $\alpha$ ),  
155 and vascular endothelial growth factor (VEGF). The sensitivity of the aforementioned cytokines  
156 in the panel ranged from 0.07 to 15.85 pg/ml. Interferon- $\gamma$  concentrations in BALF were also  
157 measured by using Mouse IFN $\gamma$  ELISA MAX<sup>TM</sup> Standard kit (BioLegend, San Diego, CA) per  
158 manufacturer's protocol.

### 159 *RNA sequencing analysis*

160 RNA sequencing was conducted at the Bauer Center Sequencing Core at Faculty of Arts and  
161 Sciences Center for Systems Biology, Harvard University. Ribo-depleted RNA was isolated  
162 from total RNA of purified murine alveolar macrophages collected on post-influenza day 9 and  
163 11. Automated library preparation was performed using the Apollo 324<sup>TM</sup> System (WaferGen  
164 Biosystems, Inc., Fremont, CA, USA) to generate a library of 100-base-pair single-end reads for  
165 RNA sequencing. DNA fragments were purified with PCRClean DX Kit from Aline Biosciences  
166 (Woburn, MA, USA). Samples were pooled in equal molar amounts, and sequenced with the  
167 Illumina HiSeq 2500 System (Illumina, Inc., San Diego, CA, USA).

168 For data filtering and mapping of reads, Trim Galore  
169 ([http://www.bioinformatics.babraham.ac.uk/projects/trim\\_galore/](http://www.bioinformatics.babraham.ac.uk/projects/trim_galore/)) was used to quality trim raw  
170 reads and adapters with a minimum quality score of 30, and minimum sequence length of 80.  
171 FASTX-Toolkit ([http://hannonlab.cshl.edu/fastx\\_toolkit/](http://hannonlab.cshl.edu/fastx_toolkit/)) was then used to remove the first 10  
172 bases. Remaining reads were mapped to the reference mouse genome from the Ensembl database  
173 using the "sensitive" preset parameters in Bowtie 2 (36). A count table of mapped reads was  
174 created for each gene, and reads per kilobase of transcript per million mapped reads (RPKM)  
175 were calculated from the Bowtie 2 output using the generalized fold change (GFOLD) algorithm

176 (17). The R package of DESeq (3) was used to identify differentially expressed genes and to  
177 calculate adjusted p values for comparisons.

178 Two replicates from each group were analyzed using QIAGEN's Ingenuity<sup>®</sup> Pathway Analysis  
179 (IPA<sup>®</sup>, QIAGEN Redwood City, USA) and MetaCore<sup>™</sup> (Thomson Reuters, USA) for  
180 identification of over-represented transcription factors and functional analysis of differentially  
181 expressed genes. The sequence data are available through the NCBI database using the accession  
182 number PRJNA311622.

183 For analysis using a Connectivity Map approach (35), we used the Touchstone database available  
184 at clue.io The top DEGs passing a filter of adjusted p value < .01 were used, resulting in  
185 submission of 476 and 428 up- and down-regulated DEGs respectively for analysis. The results  
186 table was sorted by percentile rank based on their ability to cause a gene expression pattern most  
187 similar to the gene signature found by comparing DEGs in day 11 vs day 9 macrophages.

#### 188 ***Quantitative reverse transcription - polymerase chain reaction***

189 Total RNA was extracted according to the manufacturer's manual using Qiagen RNeasy Micro  
190 Kit (Valencia, CA, USA). For each sample of FACS-sorted mouse alveolar macrophages, 150 ng  
191 of RNA was reverse transcribed into cDNA using *Applied Biosystems*<sup>®</sup> High Capacity cDNA  
192 Reverse Transcription Kits (Grand Island, NY, USA). For each sample of AM-MDMs or THP-1  
193 cells, 1 µg of RNA was reverse transcribed. The quantitative reverse transcription – PCR (qRT-  
194 PCR) was performed on an *Applied Biosystems*<sup>®</sup> 7300 *Real Time PCR* System with  
195 amplification cycles of 95°C for 10 minutes, 40 cycles of 95°C for 10 seconds, 60°C for 30  
196 seconds, and 72°C for 10 seconds.

197 ***Immunoblot analysis***

198 AM-MDMs were washed with cold phosphate-buffered saline and lysed with protease and  
199 phosphatase inhibitors in 1% NP-40 lysis buffer for 30 minutes on ice. Cell lysates were  
200 resolved on NuPAGE® Novex® 4-12% Bis-Tris Protein Gels (Life Technologies, Grand Island,  
201 NY, USA), and transferred to nitrocellulose membranes. Antibodies used for immunoblot  
202 analysis included from Cell Signaling: phosphor-Akt (Ser 473, **Rabbit mAb #4060**), Akt  
203 (**Rabbit mAb #4685**), and  $\beta$ -Actin; polyclonal rabbit anti-MARCO, sc-68913, was obtained  
204 from Santa Cruz Biotechnology. Immunoreactive bands were detected by chemiluminescence.  
205 Densitometric analysis of the immunoblots was performed using ImageJ (National Institutes of  
206 Health).

207 ***Stable transduction of THP1 cells***

208 MISSION® Lentiviral Transduction Particles with human TFEB shRNA (Sigma-Aldrich, St.  
209 Louis, MO, USA) or human TFEB (BC032448.1) ORF cDNA lentiviral particles (GeneCopoeia,  
210 Rockville, MD, USA) were added to  $1 \times 10^6$  human THP-1 cells at a MOI of 0.3 after cells were  
211 incubated in  $5 \mu\text{g/ml}$  hexadimethrine bromide for 10 minutes. Cells were then spun at  $1,000 \times g$   
212 for 90 minutes at  $30^\circ\text{C}$ , and incubated at  $37^\circ\text{C}$  for 5 hours before fresh RPMI-1640 media was  
213 added. Following overnight incubation at  $37^\circ\text{C}$ , cells were washed and grown in culture media  
214 containing puromycin  $5 \mu\text{g/ml}$ .

215 ***Transfection of human monocyte-derived macrophages***

216 AM-MDMs were transfected with ON-TARGETplus Human TFEB siRNA or ON-TARGETplus  
217 Non-targeting Pool (GE Healthcare Dharmacon, Inc., Lafayette, CO, USA) using PolyJet™

218 DNA In Vitro Transfection Reagent (SignaGen Laboratories, Rockville, MD, USA) according to  
219 the manufacturer's protocol.

### 220 ***Mouse model of post-influenza bacterial pneumonia***

221 Eight-to-nine-week-old MARCO *-/-* (4) or wild-type control male mice on a C57BL/6  
222 background (Jackson Laboratory, Bar Harbor, ME) were used in the *in vivo* model of post-  
223 influenza bacterial pneumonia. Animals were cared for in accordance with the Institutional  
224 Animal Care and Use Committee (IACUC) guidelines. Experimental procedures on animals  
225 were conducted after approval by the Harvard Medical Area (HMA) Standing Committee on  
226 Animals. For the post-influenza pneumonia model, mice were intranasally inoculated with 1 PFU  
227 of influenza virus strain A/Puerto Rico/8/34 (PR8) (Virasource, Raleigh-Durham, NC) per  
228 mouse in 25  $\mu$ l PBS after anesthesia with ketamine (200 mg/kg) and xylazine (20 mg/kg). On  
229 day 7 after influenza infection, mice were intranasally infected with 300 to 500 CFUs of *S.*  
230 *pneumoniae* serotype 3 in 25  $\mu$ l PBS after anesthesia. Body weight and morbidity were  
231 monitored after infections.

### 232 ***Scanning cytometry analysis of MARCO expression and bacterial uptake***

233 For analysis of treatment effects on MARCO expression, AM-MDMs were incubated with mAbs  
234 PLK-1 (5) or IgG3 isotype control at 4°C after Fc receptor blockade. Cells were then washed and  
235 stained with Alexa Fluor® 594 F(ab')<sub>2</sub> fragment of goat anti-mouse IgG (Invitrogen™, Grand  
236 Island, NY, USA). Dead cells were stained with the Invitrogen™ LIVE/DEAD Fixable Green  
237 Dead Cell Stain Kit per manufacturer's instructions. After fixation with 4% formaldehyde, cells  
238 were stained with Hoechst nuclear stain and CellMask blue stain (Invitrogen™, Grand Island,  
239 NY, USA).

240 For analysis of treatment effects on AM-MDM uptake of GFP-labeled bacteria,  
241 extracellular bacteria were stained with Alexa Fluor 594–labeled monoclonal antibody to *S.*  
242 *aureus* (ABIN4356218, Novus Biologicals), or lysed with lysostaphin (20 µg/ml, 30 min). For  
243 MARCO inhibition experiments, cells were incubated in 200 µg/ml of polyinosinic acid  
244 (poly(I)), a class A scavenger receptor inhibitor, at 37°C for 30 minutes prior to bacterial  
245 infection. Alternatively, GFP-*S. aureus* suspensions were incubated with or without MARCO  
246 blocking peptides (Santa Cruz Biotechnology, Inc., Dallas, Texas, USA) for 30 minutes prior to  
247 infection. Dead cells were stained with the Invitrogen™ LIVE/DEAD Fixable Red Dead Cell  
248 Stain Kit. After fixation with 4% formaldehyde, cells were stained with Hoechst nuclear stain  
249 and CellMask blue stain (Invitrogen™, Grand Island, NY, USA).

250 Scanning cytometry BD Pathway 855 High-Content Bioimager (BD Biosciences, San  
251 Jose, CA, USA) was used to acquire confocal fluorescence images of MARCO surface labeling  
252 and binding and uptake of bacteria, and image data were analyzed using MATLAB® image  
253 analysis software (13).

#### 254 ***Fluorescence-activated cell sorting (FACS)***

255 Cells collected from BAL on day 3, 5, 7, 9, and 11 after influenza infection of C57BL/6 mice  
256 were stained with fluorescein isothiocyanate (FITC)–conjugated anti-MARCO antibodies (AbD  
257 Serotec, Raleigh, NC, USA), Alexa Fluor 647-conjugated F4/80 antibodies (BioLegend, San  
258 Diego, CA), PE-Cy7-conjugated CD11c<sup>+</sup> antibodies (BioLegend, San Diego, CA), and their  
259 corresponding isotypes after Fc Receptor blockade. F4/80<sup>+</sup>CD11c<sup>+</sup> cells were sorted using the  
260 BD *FACSAria™ II cell sorter* (BD Biosciences, San Jose, CA, USA) for RNA extraction.

#### 261 ***Chromatin immunoprecipitation (ChIP)***

262 The SimpleChIP<sup>®</sup> Enzymatic Chromatin IP Kit (Magnetic Beads) #9003 from Cell Signaling  
263 Technology, Inc. (Danvers, MA) was used for chromatin immunoprecipitation according to the  
264 manufacturer's protocol. Briefly, AM-MDMs were formalin-fixed, treated with micrococcal  
265 nuclease, and sonicated. Chromatin from the AM-MDMs was immunoprecipitated with anti-  
266 TFEB antibody and its corresponding isotype (Cell Signaling Technology, Inc., Danvers, MA).  
267 Immunoprecipitated nuclear DNA was extracted, and analyzed by PCR with primers targeting  
268 the human MARCO upstream promoter area. The MARCO primers used for the ChIP assay  
269 were: forward, 5'-CCCTGGTAGAGATGCCTGAC-3'; reverse, 5'-  
270 GAAGCCTTGCTCTGAACCAC-3'.

#### 271 *Statistical analysis*

272 Statistical analyses were performed using GraphPad Prism 6 (GraphPad Software, Inc., San  
273 Diego, CA). Results are expressed as the mean  $\pm$  standard deviation (SD). Student's t-test was  
274 performed to compare treatment effects between two groups, and one-way analysis of variance  
275 (ANOVA) with Bonferroni adjustment for comparison between multiple groups. Mortality of  
276 mice was analyzed by the Kaplan-Meier and log-rank methods.

277

278

279 **Results**

280 ***MARCO mRNA expression of sorted alveolar macrophages after influenza virus infection***

281 Lung cells from influenza-infected mice were collected by lavage on days 3, 5, 7, 9, and 11 after  
282 infection. Lavaged F4/80+CD11c+ cells were sorted as alveolar macrophages (6, 34) (Figure  
283 1A), and *Marco* expression was measured by qRT-PCR. Corresponding to the increased IFN $\gamma$   
284 levels on post-influenza days 7 and 9 (Figure 1B), *Marco* expression was down-regulated on  
285 days 7 (0.46 fold,  $p < 0.0001$ , Figure 1C) and 9 (0.51 fold,  $p < 0.0001$ ). However, there was a  
286 surprising 4.86-fold increase ( $p < 0.0001$ ) in *Marco* expression between day 9 and 11. Moreover,  
287 *Marco* expression was up-regulated 2.48 fold ( $p < 0.0001$ ) on day 11 compared to un-infected  
288 controls.

289 To explore the basis for these changes in *Marco* expression, levels of large panel of  
290 cytokines were measured in lavage fluids using a multiplexed array assay. The results are  
291 summarized in Figure 2 and identified several cytokines whose expression declines from day 7  
292 onward. Consistent with prior studies (73), IFN $\gamma$  exhibited the greatest increase on day 7  
293 compared to day 5 (261-fold), and also when day 7 was compared to days 9 or 11 (524-fold and  
294 66-fold, respectively). A subset of the cytokines assayed showed a similar pattern (e.g., IL-4, 10,  
295 12p70, fold-change data not shown), but no single cytokine showed a unique change in  
296 magnitude or pattern that might easily explain (by itself) the marked increase in *Marco*  
297 expression between day 9 and 11.

298

299 ***RNA sequencing analysis of sorted alveolar macrophages on day 9 and 11 after influenza***  
300 ***infection***

301 To explore potential mechanisms for up-regulation of *Marco* expression more broadly, RNAseq  
302 analysis was performed on F4/80+CD11c+ alveolar macrophages purified by flow sorting from  
303 mice on post-influenza days 9 and 11. 1537 differentially expressed genes (DEGs) were  
304 identified between day 9 and day 11 samples, using criteria of adjusted  $p < 0.01$ ; (Table S1).  
305 Notably, these included Marco, v-akt murine thymoma viral oncogene homolog 1 (Akt1 or Akt),  
306 mitogen-activated protein kinase 3 (Mapk3), and another Nrf2-regulated gene, heme oxygenase  
307 1 (Hmox1). Enrichment analysis using MetaCore™ showed that the candidate genes were  
308 associated with process networks relevant to the resolution phase of influenza (Table S2), and  
309 also showed that NRF2 and TFEB are among the most over-represented transcription factors  
310 (based on binding sites in genes differentially expressed in AMs between day 9 and day 11,  
311 Table S3). Finally, analysis of the DEGs using the CLUE portal to query the Connectivity Map  
312 Touchstone dataset (clue.io/touchstone) identified agents that cause gene expression changes that  
313 correlate strongly with the gene signature linked to up-regulated MARCO on day11. Six of the  
314 top 10 compounds (out of the 2,837 compounds evaluated) activate NRF2 (by rank: 1) celastrol  
315 (16), 5 & 6) topoisomerase inhibitors SN38 and topotecan (54), 7) mycophenolate (75) 8)  
316 triptolide (90), 9) trichostatin (9)) We further investigated immunomodulation of both of these  
317 targets, focusing on sulforaphane activation of NRF2 (47) and Akt-mediated activation of TFEB.

318

### 319 ***Sulforaphane increases MARCO expression of IFN $\gamma$ -treated human macrophages***

320 To model the effects of influenza *in vitro*, we treated primary AM-MDMs with IFN $\gamma$  for 24  
321 hours, which resulted in down-regulation of MARCO expression, (0.54 $\pm$ 0.20 fold change vs.  
322 control,  $p < 0.001$ , Figures 3A and 3B). SFN treatment up-regulated MARCO expression and  
323 diminished the IFN $\gamma$ -mediated reduction in MARCO expression (0.92 $\pm$ 0.25 vs. 0.54 $\pm$ 0.20 fold

324 change,  $p < 0.01$ ). Cell death following  $\text{IFN}\gamma$  treatment was also significantly reduced in SFN-  
325 treated groups (SFN = 10  $\mu\text{M}$ ) compared to untreated controls ( $1.3 \pm 1.5\%$  vs.  $4.5 \pm 2.0\%$ ,  $p < 0.01$ ,  
326 Figures 3A and 3C). Similarly, treatment of differentiated human THP-1 macrophages with  $\text{IFN}\gamma$   
327 (5 – 50 IU/ml) resulted in a dose-dependent down-regulation of MARCO expression and  
328 increased cell death, which were reversed by treatment with SFN (Figs. 4A & B).

329

330 ***Sulforaphane improves bacterial phagocytosis in  $\text{IFN}\gamma$ -treated AM-MDMs through MARCO***  
331 ***upregulation***

332 AM-MDMs were challenged with *S. aureus* following ~24 hours of  $\text{IFN}\gamma$  pre-treatment.  
333 Phagocytosis of fluorescent GFP-labeled *S. aureus* by AM-MDMs was impaired by  $\text{IFN}\gamma$   
334 treatment ( $p < 0.05$ , Figures 3D, 3E, and 3F), but significantly improved when treated  
335 simultaneously with SFN ( $p < 0.01$ ). Cell death following  $\text{IFN}\gamma$  and *S. aureus* infection was also  
336 reduced by concurrent SFN treatment (data not shown).

337 To further delineate the causal link between sulforaphane treatment, MARCO expression,  
338 and bacterial phagocytosis, we treated AM-MDMs with either the broad class A scavenger  
339 receptor blocker, polyinosinic acid [poly(I)], or a specific MARCO blocking peptide prior to *S.*  
340 *aureus* infection. The rescue effect of SFN on bacterial phagocytosis after  $\text{IFN}\gamma$  treatment was  
341 significantly inhibited by both poly(I) (5.19 bacteria per cell, 95% CI 2.62 to 7.76, vs. 3.25, 95%  
342 CI 0.47 to 6.04,  $p < 0.01$ , Figure 3E) and the specific MARCO blocking peptide (5.21, 95% CI  
343 4.39 to 6.02, vs. 3.04, 95% CI 1.75 to 4.33,  $p < 0.05$ , Figure 3F). Taken together with the previous  
344 findings these results indicate that SFN improves bacterial phagocytosis in  $\text{IFN}\gamma$ -treated  
345 macrophages through up-regulation of the class A scavenger receptor MARCO. In contrast to  
346 uniform results seen with the THP-1 cell line, considerable donor-to-donor variability was seen

347 with primary AM-MDM cells. However, AM-MDMs from all donors showed a similar pattern,  
348 with IFN $\gamma$  causing a reduction in bacterial phagocytosis that was reversed by SFN, and MARCO  
349 blockade resulting in inhibition of phagocytosis that was not abrogated by SFN (Figure 3E and  
350 3F).

351 We also tested the effects of another Nrf2 activator, epigallocatechin gallate (EGCG) (24,  
352 86), on MARCO expression and bacterial phagocytosis in AM-MDMs from 2 donors. EGCG  
353 also reversed declines in MARCO expression and *S. aureus* phagocytosis caused by IFN $\gamma$   
354 (Figure 5).

355

### 356 *Sulforaphane improves bacterial clearance and host survival in post-influenza bacterial* 357 *pneumonia*

358 We investigated the effects of SFN using the *in vivo* model of post-influenza bacterial  
359 pneumonia summarized schematically in Fig. 6A. To study the effects of SFN on bacterial  
360 clearance, mice were subcutaneously injected with SFN or vehicle on post-influenza days 6 to 9  
361 (i.e. day -1 to 2 post *S. pneumoniae* infection). SFN treatment significantly improved clearance  
362 of *S. pneumoniae*, measured as bacterial colony forming units (CFU) in bronchoalveolar lavage  
363 fluid, compared to untreated controls ( $\log_{10}$  CFU =  $6.09 \pm 0.60$  vs.  $7.57 \pm 0.20$ ,  $p=0.036$ , Figure  
364 6B). To study the effects of SFN on host survival in post-influenza bacterial pneumonia, mice  
365 were injected with SFN or vehicle on post-influenza days 6 to 9 or 10 (i.e. day -1 to 2 or 3 post *S.*  
366 *pneumoniae* infection) (Figure 6A). SFN-treated mice exhibited lower body weight loss and  
367 faster weight recovery after post-influenza bacterial infection compared to controls (data not  
368 shown). Notably, SFN improved survival in wild-type (53.3% vs. 5.9%,  $p<0.0001$ , Figure 6C)  
369 but not *Marco*<sup>-/-</sup> mice (Figure 6D), indicating that *Marco* expression was required for the

370 beneficial effect of SFN. Median survival times for SFN-treated and vehicle-treated wild-type  
371 mice were >12 days and  $4.7 \pm 0.2$  days, respectively.

372

373

374 ***Role of Akt activation on MARCO expression and bacterial phagocytosis in post-influenza***  
375 ***bacterial pneumonia.***

376 Akt and MAPK3 were among the top five genes identified as enriched network objects analysis  
377 from the Metacore analysis of the RNAseq results (in order, with # of networks involved:  
378 ERK1/2 (33), MAPK3 (30), PI3KIA (29), AKT (27), NF-kB (24)). Both were also previously  
379 found to be altered by influenza (18). qRT-PCR showed that *Akt* and *Mapk3* mRNA expression  
380 levels in murine alveolar macrophages gradually declined after influenza infection (Figures 7A  
381 and 7B), but were increased on post-influenza day 11 compared to the reduced levels from day 5  
382 to day 9. The nadirs of *Akt* and *Mapk3* expression occurred on day 7 and day 9, respectively.  
383 These patterns of *Akt* and *Mapk3* expression were concordant with that of MARCO expression,  
384 and inversely corresponded to IFN $\gamma$  levels in BALF.

385 Both Akt inhibitor perifosine (10 to 50  $\mu$ M) (26, 74) (Figure 8A) and MAPK/ERK  
386 inhibitors U0216 and PD98059 (2, 53) (data not shown), reduced MARCO expression on AM-  
387 MDMs supporting a role for Akt and MAPK signaling pathways in MARCO expression in  
388 human macrophages.

389 Western blot analysis of AM-MDMs showed that IFN $\gamma$  treatment decreased both pAkt  
390 and MARCO. Moreover, treatment with the Akt activator SC79 (30) increased MARCO levels  
391 in the presence of IFN $\gamma$  (Figure 8B). Scanning cytometry also showed that the SC79 increased  
392 MARCO expression in IFN $\gamma$ -treated AM-MDMs ( $p < 0.001$ ,  $n = 6$ , Figures 8C and 8D). Treatment

393 with MAPK/ERK activators failed to change MARCO expression (data not shown). Since the  
394 available MAPK activators did not increase MARCO expression *in vitro*, we chose to focus on  
395 Akt. SC79 treatment increased phagocytosis of GFP-*S. aureus* by IFN $\gamma$ -treated AM-MDMs  
396 (Figure 9A and 9B). Finally, the rescue effect of SC79 in increasing bacterial phagocytosis was  
397 significantly inhibited by the class A scavenger receptor, poly(I) (Figure 9C).

398 To study the effects of SC79 on *in vivo* survival from secondary pneumonia, mice were  
399 treated with SC79 (20 mg/kg) or vehicle from days 6 to 9 or 10 (i.e. day -1 to day 2 or 3 post *S.*  
400 *pneumoniae* infection) (Figure 9D). SC79-treated mice had a significantly higher survival rate  
401 compared to vehicle-treated mice (25% vs. 4%,  $p=0.001$ , Figure 9E). The median survival times  
402 for SC79-treated and vehicle-treated mice were  $6.8 \pm 1.1$  and  $4.9 \pm 0.3$  days, respectively.

403

#### 404 ***TFEB is an over-represented transcription factor regulating susceptibility to post-influenza*** 405 ***bacterial pneumonia***

406 Since TFEB, the most over-represented transcription factor in our transcriptome data, was also  
407 recently identified as an important regulator of innate immunity in *C. elegans* and in murine  
408 macrophages (83), we investigated the role of TFEB in our post-influenza model. TFEB is  
409 known to translocate to the nucleus and bind to E-box sequences (5'-CANNTG-3') (69).  
410 Examination of the MARCO promoter region (-2,000 to +200) showed multiple E-box  
411 sequences, and thus potential binding sites for TFEB (Figure 10). To investigate whether TFEB  
412 binds to the MARCO promoter, AM-MDMs were subjected to chromatin immunoprecipitation  
413 using anti-TFEB antibody. PCR with primers targeting the upstream sequence (-824 to -622) of  
414 human MARCO gene showed enhanced detection, consistent with binding of TFEB to the  
415 MARCO promoter area (Figure 11A).

416 A possible association between MARCO, Akt, and TFEB is suggested by the findings  
417 that increased mTORC1 activity down-regulates Akt activity and MARCO expression (78, 87),  
418 and sequesters TFEB in the cytoplasm through phosphorylation (59). We used RNA interference  
419 to knock down TFEB in THP-1 macrophages and AM-MDMs prior to treatment with the Akt  
420 activator SC79 (30). THP-1 cells stably transduced with lentivirus-delivered shRNA against  
421 TFEB showed an almost five-fold reduction in MARCO mRNA expression ( $p=0.002$ , Figure  
422 11B) and a seventy-percent reduction in *Hmox1* (data not shown) compared to cells transduced  
423 with non-targeting shRNA. Mouse B6 cells (derived from alveolar macrophages) transduced  
424 with shRNA against TFEB also showed reduced *Marco* mRNA expression compared to non-  
425 targeting shRNA-transduced controls (data not shown). In contrast, after lentiviral transduction,  
426 TFEB-overexpressing THP-1 cells showed a >300-fold increase in *Marco* expression ( $p<0.0001$ ,  
427 Figure 11C) and a five-fold increase in *Hmox1* expression (data not shown). To test the effect of  
428 TFEB levels on the interaction of Akt and MARCO expression, we treated TFEB knockdown  
429 cells with the Akt activator SC79. SC79-induced MARCO expression in IFN $\gamma$ -treated  
430 macrophages was abrogated in primary AM-MDMs transfected with TFEB siRNA ( $p<0.01$ ,  $n=5$ ,  
431 Figures 11D and 11E), and in THP-1 knockdowns (data not shown), suggesting a link between  
432 Akt signaling, TFEB nuclear translocation, and MARCO expression (Figure 12).

433

434

435 **Discussion**

436 Alveolar macrophages are critical for maintaining lung homeostasis and promoting  
437 survival following influenza infection (12, 20, 62), including defense against secondary  
438 pneumonia. We investigated the role of the AM scavenger receptor MARCO in these defenses to  
439 identify potential immunomodulators that could be used to reduce the risk of post-influenza  
440 bacterial pneumonia. Initially, elevated IFN $\gamma$  levels following influenza infection corresponded  
441 to synchronous decreases in AM MARCO expression. However, as IFN $\gamma$  levels returned to  
442 normal on post-influenza day 11, there was a striking increase in MARCO expression.  
443 Transcriptome profiling of purified lung macrophages indicated important roles for NRF2 and  
444 Akt/TFEB-related signaling in the unexpectedly high rebound level of MARCO. High levels of  
445 IFN $\gamma$  after influenza virus infection correlated with decreased MARCO expression *in vivo* and  
446 caused impaired phagocytosis in AM-MDMs *in vitro*. Activating the Nrf2 and Akt signaling  
447 pathways with sulforaphane and SC79, respectively, increased MARCO expression and  
448 improved bacterial phagocytosis in the presence of IFN $\gamma$ . In an *in vivo* model of post-influenza  
449 bacterial pneumonia, both SC79 and sulforaphane improved host survival. The sulforaphane-  
450 induced improvement of survival was observed in wild-type but not in MARCO knockout mice,  
451 suggesting that MARCO is an indispensable mediator for Nrf2 effects in post-influenza bacterial  
452 pneumonia.

453 Some limitations of our study merit discussion. Although previous studies have shown  
454 that GM-CSF-matured human macrophages (AM-MDMs) used on our *in vitro* studies resemble  
455 primary AMs by numerous criteria, (13, 71), and IFN $\gamma$  treatment of AM-MDMs reproduces the  
456 post-influenza down-regulation of lung macrophage MARCO expression and impaired bacterial  
457 phagocytosis seen *in vivo*, it is possible that responses of true primary lung macrophages may

458 differ. In addition, although our mouse model of post-influenza is similar to that used by many  
459 other investigators (20, 28, 41, 67, 68, 72), results may be dependent upon influenza dose as well  
460 as the dose and type of bacteria used for secondary infection (29, 38, 45, 70). In our secondary  
461 model we did not measure viral load on day 7, the day of secondary bacterial infection. In studies  
462 using much higher inocula of virus (designed to cause primary influenza pneumonia), we  
463 observed a marked decrease in viral load by day 6 (21). Here, with a much lower inoculum that  
464 causes minimal inflammation and weight loss, it is likely that virus is cleared by day 7. However,  
465 whether there remains some residual virus has not been directly addressed in our data. We  
466 focused on IFN $\gamma$ -mediated effects but our multiplex cytokine results could be interpreted as  
467 showing that changes in the levels of several other cytokines (individually or in combinations)  
468 may contribute to the striking increase in MARCO levels from day 9 to 11. Another issue that  
469 merits mention is our use of *S. aureus* for in vitro studies, while the in vivo studies use *S.*  
470 *pneumoniae*. Both pathogens are common agents in secondary post-influenza pneumonia, and  
471 both are engaged by MARCO and other scavenger receptors. However, in vivo secondary  
472 pneumonia models using pneumococcus may be more relevant since they require much lower  
473 inocula (e.g. 500 CFU), whereas inocula of 10<sup>8</sup> are commonly required for post-influenza studies  
474 with *S. aureus*. Moreover, using the GFP-*S. aureus* in vitro allowed the use of fluorescent assays  
475 reported, a strategy not possible for pneumococcus given the lack of available fluorescence  
476 tagged *S. pneumoniae*. Future studies with both in vitro and in vivo analyses using the same  
477 organism could add to understanding of any pathogen-specific aspects. Finally, there is a rich  
478 literature that identifies multiple mediators as causal for post-influenza secondary pneumonia (8,  
479 15, 22, 31-33, 38, 40, 42, 44, 52, 55-58, 72, 79, 82, 85), including type I interferons (37). The

480 proposed multiple mechanisms are not necessarily mutually exclusive, and may offer alternative  
481 targets for immunomodulator interventions.

482 Notably, we found that the MARCO rescue effect of Akt activation is dependent upon the  
483 transcription factor TFEB, a lysosome and autophagy master regulator. These results are  
484 congruent with previous studies in which PI3K inhibitors reduced scavenger receptor-mediated  
485 phagocytosis (71). The class A scavenger receptor inhibitor poly(I) blocked the SC79-mediated  
486 increase in bacterial phagocytosis, indicating a link between Akt signaling and scavenger  
487 receptors. It has previously been shown that IFN $\gamma$  produced by influenza infection induces  
488 hyper-activated mTORC1 (87), which in turn inhibits Akt activity (10), and reduces both  
489 MARCO expression and unopsonized phagocytosis (87). It is also possible that IFN $\gamma$  inhibits  
490 Akt activity through undiscovered mTORC1-independent pathways. Taken together, these data  
491 suggested that IFN $\gamma$  production after influenza is associated with attenuated Akt signaling and  
492 MARCO expression in alveolar macrophages. The rebound phenomenon of MARCO expression  
493 on post-influenza day 11 may be due to a feedback-based increase of Akt activity from the  
494 previously inhibited state. It is worth noting that the magnitude of changes in Akt expression  
495 (Fig. 7A) is relatively small. Moreover, phosphorylation state rather than expression level often  
496 regulates Akt activity. Future studies are warranted to further delineate these potentially  
497 important details.

498 Notably, both TFEB and Nrf2 are among the over-represented transcription factors  
499 regulating differentially expressed genes during the recovery period of post-influenza MARCO  
500 expression (Table S3), indicating that both are essential in restoration of homeostasis and/or host  
501 defense against post-influenza complications. There may be some interplay between these two  
502 transcription factors since: 1) as we have shown here, TFEB mediates Akt signaling in MARCO

503 upregulation; 2) activation of either insulin receptor (84) or epidermal growth factor receptor  
504 tyrosine kinase (48) induces Nrf2 activation through PI3K/Akt signaling; 3) PI3K/Akt signaling  
505 pathway may be activated by sulforaphane, leading to increased expression of Nrf2-regulated  
506 genes (14, 39); 4) THP-1 cells stably transduced with shRNA against TFEB showed reduced  
507 expression of *Hmox1*, an Nrf2-regulated gene, compared to the non-targeting shRNA control,  
508 whereas TFEB-overexpressing THP-1 cells showed increased *Hmox1* expression when  
509 compared to the control. We speculate that the ability of sulforaphane to also reverse IFN $\gamma$ -  
510 mediated cell death (Figs. 3C, 4A) may also reflect activation of pro-survival Akt signaling, but  
511 our data do not directly test this postulate. Taken together, these data suggest that TFEB, Nrf2,  
512 and MARCO expression are correlated with each other and all associated with Akt signaling.

513         The mechanism(s) by which MARCO expression is inhibited by IFN $\gamma$  is unclear.  
514 Previous data showed that tyrosine kinases, protein kinase C, PI3K signaling, and MAPK  
515 pathway are involved in macrophage scavenger receptor-mediated phagocytosis (71).  
516 Interactions between Nrf2 and PI3K Akt signaling are known (48, 84). These data indicate that  
517 Nrf2 signaling and regulation of MARCO expression are both coupled to the MAPK and  
518 PI3K/Akt signaling pathways, but the specific pathways for IFN $\gamma$  effects need further  
519 characterization.

520         Figure 12 summarizes our working hypotheses regarding the role of TFEB in mediating  
521 Akt-dependent signaling to upregulate MARCO, the major opsonin-independent phagocytic  
522 receptor on alveolar macrophages, in the post-influenza alveolar milieu. Our data also suggest  
523 that expression of the scavenger receptor MARCO may be linked to additional TFEB-regulated  
524 autophagy and/or lysosomal genes. Our results show that, in addition to Nrf2, Akt signaling and  
525 TFEB may be effective therapeutic targets in post-influenza bacterial pneumonia.

526 **Funding:** This work was supported by NIH ES00002, and HL115778

527 **Figure Legends**

528

529 **Figure 1. MARCO expression is spontaneously restored and increased in the later phase of**  
530 **influenza virus infection.**

531 (A) Bronchoalveolar lavage samples were collected after influenza infection, and  
532 F4/80+CD11c+ cells (alveolar macrophages) were sorted and subjected to RNA  
533 extraction and qRT-PCR for evaluation of *MARCO* expression.

534 (B) ELISA of bronchoalveolar lavage fluids collected from influenza-infected mice showed  
535 that IFN $\gamma$  levels significantly increased on day 7 and day 9 compared to uninfected  
536 controls. N = 3-5 per group.

537 (C) Quantitative RT-PCR of sorted alveolar macrophages showed that *MARCO* expression  
538 was down-regulated on day 7 ( $p < 0.0001$ ) and day 9 ( $p < 0.0001$ ) post-influenza virus  
539 infection, but up-regulated on day 11 ( $p < 0.0001$ ) compared to uninfected controls. N= 3-  
540 9 per group. Data are shown as fold change after normalization to the housekeeping gene  
541 *TBP* expression; for both B, C: p values: \* $< 0.05$ , \*\* $< 0.01$ , \*\*\* $< 0.001$ , or \*\*\*\* $< 0.0001$ .

542

543 **Figure 2. Cytokine multiplex assay of bronchoalveolar lavage fluids from influenza-**  
544 **infected C57BL/6 mice.**

545

546 Day 0: uninfected control; D3, D5, D7, D9, D11: post-influenza day 3, 5, 7, 9, 11. There were  
547 three mice in each group, represented by individual symbols; columns show mean values.

548

549

550

551

552

553 **Figure 3. Sulforaphane significantly improves MARCO expression, bacterial phagocytosis,**  
554 **and reduces cell death in IFN $\gamma$ -treated human monocyte-derived macrophages.**  
555

556 **(A)** Representative images of scanning cytometry analysis of AM-MDMs after treatment with  
557 IFN $\gamma$  and/or SFN. Red, MARCO on the cell surface; green, dead cells.

558 **(B)** Quantitation of results of scanning cytometry analysis of AM-MDMs treated with or  
559 without IFN $\gamma$  and SFN. Fluorescence index (FI) = % positive x mean fluorescence  
560 intensity of all cells (MFI). Number of donors = 6. Data are represented as mean  $\pm$  SD.

561 **(C)** SFN treatment reduced cell death in IFN $\gamma$ -treated AM-MDMs. Number of donors = 6.  
562 Data are represented as mean  $\pm$  SD.

563 **(D)** Representative images of scanning cytometry analysis of AM-MDMs after treatment with  
564 IFN $\gamma$  and/or SFN, followed by GFP-*S. aureus* infection. Extracellular bacteria were  
565 labeled with red-fluorescent dye.

566 **(E)** Individual donor results showing decreased phagocytosis in response to IFN $\gamma$ ,  
567 improvement by SFN, and blockade of SFN-effect with the scavenger receptor inhibitor,  
568 poly(I). Number of donors = 6. Colors indicate different donors.

569 **(F)** Individual donor results showing decreased phagocytosis in response to IFN $\gamma$ ,  
570 improvement by SFN, and blockade of SFN-effect with the MARCO peptide for  
571 competition studies. Number of donors = 6. Colors indicate different donors. for B, C, E,  
572 F: p values: \* $<$  0.05, \*\* $<$ 0.01, \*\*\* $<$ 0.001.

573

574

575

576

577 **Figure 4. Sulforaphane significantly improves MARCO expression and reduces cell death**  
578 **in IFN $\gamma$ -treated THP1 macrophages.**

579 **(A)** Scanning cytometry analysis showed that IFN $\gamma$  reduced MARCO expression on THP1 cells  
580 in a dose-dependent manner, but simultaneous treatment with sulforaphane upregulated and/or  
581 restored MARCO expression in IFN $\gamma$ -treated THP1 cells. Fluorescence index (FI) of MARCO  
582 expression = % of THP1 cells expressing MARCO x MFI (mean fluorescence intensity of all  
583 cells). Data represent means of four replicates from two independent experiments.

584 **(B)** SFN treatment also reduced cell death in the IFN $\gamma$ -treated THP1 cells.

585

586

587 **Figure 5. Epigallocatechin gallate (EGCG) increases MARCO expression and bacterial**  
588 **phagocytosis in IFN $\gamma$ -treated cells.**

589 **(A)** The Nrf2 activator, EGCG, improved MARCO expression in IFN $\gamma$ -treated AM-MDMs.  
590 AM-MDMs were incubated with or without of IFN $\gamma$  (20, 50 IU/ml) and EGCG (50 $\mu$ M). Data  
591 shown are mean fold-changes in MFI (mean fluorescence intensity) in cells from 2 donors.

592 **(B)** EGCG improved phagocytosis of GFP-*S. aureus* in IFN $\gamma$ -treated macrophages. Fluorescence  
593 index (FI) of phagocytosis = % of cells with phagocytosed bacteria x number of bacteria per cell.

594

595 **Figure 6. Sulforaphane improves clearance of *S. pneumoniae* and host survival in wild-type**  
596 **C57BL/6 mice with post-influenza bacterial pneumonia.**

597 **(A)** Summary of secondary pneumonia model starting infection with influenza virus strain  
598 A/Puerto Rico/8/34 (PR8) on day 0, followed by *S. pneumoniae* infection on day 7. Mice  
599 received daily treatments with either vehicle or sulforaphane from post-influenza day 6 to  
600 day 9 or 10.

601 (B) Treatment with SFN significantly improved bacterial clearance measured as CFU in  
602 bronchoalveolar lavage fluids on day 9 in post-influenza pneumococcal pneumonia ( $p =$   
603 0.036).

604 (C) Survival studies of wild-type C57BL/6 mice and (D) *MARCO* knockout mice with post-  
605 influenza bacterial pneumonia. Sulforaphane significantly improved host survival in  
606 wild-type mice ( $p < 0.0001$ ), but not that of *MARCO* knockouts. Number of vehicle-treated  
607 wild-type mice = 34, number of SFN-treated wild-type mice = 30, number of vehicle-  
608 treated *MARCO* knockouts = 20, number of SFN-treated *MARCO* knockouts = 20.

609

610

611

612

613 **Figure 7. Influenza infection and decreased expression of Akt and MAPK3.**

614 Numbers in the X axis indicate days after PR8 influenza virus infection in wild-type adult male  
615 C57BL/6 mice.

616 (A) Quantitative RT-PCR of sorted alveolar macrophages showed that *Akt* expression was  
617 significantly down-regulated on day 5 to day 9 post-influenza virus infection, but there was no  
618 significant difference on day 11 compared to uninfected controls. There were three to five mice  
619 in each group. Data are represented as mean  $\pm$  SD.

620 (B) Quantitative RT-PCR of sorted alveolar macrophages showed that *MAPK3* expression was  
621 significantly down-regulated on day 5 to day 9 post-influenza virus infection. The level of  
622 *MAPK3* expression significantly increased on day 11 from day 9, though it was still lower than  
623 controls. There were three to five mice in each group. Data are represented as mean  $\pm$  SD; for  
624 both A, B:  $p$  values: \* $< 0.05$ , \*\* $< 0.01$ , \*\*\* $< 0.001$ , or \*\*\*\* $< 0.0001$ .

625 **Figure 8. Akt signaling is involved in post-influenza MARCO expression.**

626 (A) MARCO expression of AM-MDMs *in vitro* (measured by scanning cytometry) is reduced  
627 by the Akt inhibitor, perifosine. Number of donors = 3. Data are represented as mean  $\pm$   
628 SD.

629 (B) AM-MDMs were treated overnight with IFN $\gamma$  (20 IU/ml) and/or SC79 (0, 2, 5, 8  $\mu$ g/ml).  
630 Western blot analysis showed that IFN $\gamma$  treatment decreased levels of MARCO. The Akt  
631 activator, SC79, increased MARCO expression in a dose-dependent manner in the  
632 presence of IFN $\gamma$ .

633 (C) Representative scanning cytometry images showed that SC79 improved MARCO  
634 expression in IFN $\gamma$ -treated AM-MDMs. AM-MDMs were treated simultaneously with 20  
635 IU/ml of IFN $\gamma$  and 8  $\mu$ g/ml of SC79 for 20 to 24 hours. Red, MARCO proteins on the cell  
636 surface; green, dead cells.

637 (D) Quantitation results of scanning cytometry analysis of AM-MDMs with or without IFN $\gamma$   
638 or SC79. Results from scanning cytometry analysis showed that Interferon- $\gamma$  treatment of  
639 human monocyte-derived macrophages reduced MARCO expression in a dose-dependent  
640 manner (data with IFN $\gamma$  10 IU/ml not shown). Fluorescence index (FI) of MARCO = %  
641 positive  $\times$  mean fluorescence intensity of each cell. Number of donors = 6. Data are  
642 represented as mean  $\pm$  SD; for both A, D: p values: \*\*<0.01, \*\*\*\*<0.0001.

643

644 **Figure 9. The Akt activator, SC79, improves AM-MDM phagocytosis of *S. aureus*.**

645 (A) Average number of phagocytosed GFP-*S. aureus* per cell after treatment with IFN $\gamma$   $\pm$   
646 SC79. SC79 treatment increased the average number of phagocytosed GFP-*S. aureus* per  
647 cell in IFN $\gamma$ -treated AM-MDMs. Number of donors = 6. Colors indicate different donors.

648 (B) Percentage of cells infected with GFP-*S. aureus* after treatment with IFN $\gamma$  and/or SC79.

649 SC79 treatment increased the proportion of cells with phagocytosed bacteria in IFN $\gamma$ -  
650 treated AM-MDMs. Number of donors = 6. Colors indicate different donors.

651 (C) The ability of SC79 to increase bacterial phagocytosis after IFN $\gamma$  treatment was  
652 significantly inhibited by the class A scavenger receptor inhibitor, poly(I). Number of  
653 donors = 4. Colors indicate different donors. for A - C: p values: \* < 0.05, \*\* < 0.01.

654 (D) Summary of secondary pneumonia model starting infection with influenza virus (PR8) on  
655 day 0, followed by *S. pneumoniae* infection on day 7. Mice received daily treatments  
656 with either vehicle or SC79 from post-influenza day 6 to day 9 or 10. Data are a  
657 combination of four independent experiments. Thirteen mice were treated with  
658 subcutaneous injection of SC79 in the dose of 20 mg/kg from post-influenza day 6 to day  
659 9. Fifteen mice received subcutaneous injection of SC79 in the dose of 20 mg/kg from  
660 post-influenza day 6 to day 10. There was no significant difference in host survival  
661 between four-day and five-day SC79 treatments.

662 (E) Survival studies of wild-type C57BL/6 mice with post-influenza bacterial pneumonia.  
663 Number of vehicle-treated mice = 25, number of SC79-treated mice = 28.

664 **Figure 10. Multiple E-box sequences are identified in the MARCO promoter area.**

665 (A) Logo representation (WebLogo 3) of the E-box sequences (CANNTG) within 2000 b.p.  
666 upstream of the transcription start site of human MARCO gene. (B) The CANNTG sites at -  
667 2000b.p. to +200b.p. of the transcription start site of the human MARCO gene. Sequences in  
668 blue indicate primers used in the ChIP assay.

669

670 **Figure 11. TFEB modulation changes MARCO expression levels.**

671 **(A)** ChIP assay of AM-MDMs ( $\pm$  treatment of SC79) showed direct binding of TFEB to the  
672 upstream promoter area of human MARCO.

673 **(B)** Relative gene expression of *TFEB* and *MARCO* in TFEB knockdown THP1 cells  
674 compared to the control transduced cells. Data are shown as fold change after  
675 normalization to the housekeeping gene *TBP* expression. Bars represent the mean and  
676 error bars represent the standard deviation of triplicates from one representative  
677 experiment of two.

678 **(C)** Relative gene expression of *TFEB* and *MARCO* in TFEB-overexpressing THP1 cells  
679 compared to control. Data are shown as fold change after normalization to the  
680 housekeeping gene *TBP* expression. Bars represent the mean and error bars represent the  
681 standard deviation of triplicates from one representative experiment of three.

682 **(D)** Representative scanning cytometry images of AM-MDMs with or without IFN $\gamma$  and/or  
683 SC79. AM-MDMs were transfected with human TFEB siRNA or non-targeting pool. NT:  
684 non-target, TFEB kd: TFEB knockdown.

685 **(E)** Quantitation results of scanning cytometry analysis of TFEB AM-MDMs knockdowns.  
686 Akt activator-induced MARCO expression in IFN $\gamma$ -treated macrophages is blocked in  
687 TFEB AM-MDM knockdowns. Fluorescence index (FI) = % positive x mean  
688 fluorescence intensity of all cells (MFI). NT: non-target, TFEB kd: TFEB knockdown.  
689 Number of donors = 5. Colors indicate different donors; for B, C, E: p values: \* $< 0.05$ ,  
690 \*\* $< 0.01$ , \*\*\* $< 0.001$ .

691

692

693 **Figure 12. TFEB mediates Akt activation-induced MARCO expression.**

694 (A) A schematic illustration depicting postulated activities between Akt, TFEB, and  
695 MARCO. Influenza infection stimulates T cell production of IFN $\gamma$ , which in turn may  
696 induce activation of mTORC1 and ensuing Akt inhibition. It is also possible that IFN $\gamma$   
697 inhibits Akt activity through mTORC1-independent pathways. Activated mTORC1  
698 sequesters TFEB in the cytoplasm, and also down-regulates MARCO expression through  
699 Akt inhibition or other downstream effectors, such as c/EBP $\beta$  inhibition (87). Akt  
700 inhibition results in MARCO down-regulation, leading to impaired bacterial phagocytosis  
701 and increased susceptibility to bacterial infection.

702 (B) Treatment with SC79 activates Akt signaling and upregulates MARCO in the presence of  
703 IFN $\gamma$  through the effects of TFEB.

704

705

706

707 **Acknowledgements:**

708 This research was supported by National Institutes of Health Grants ES00002 and HL115778.

709

710  
711  
712  
713  
714  
715  
716  
717  
718  
719  
720  
721  
722  
723  
724  
725  
726  
727  
728  
729  
730  
731  
732  
733  
734  
735  
736  
737  
738  
739  
740  
741  
742  
743  
744  
745  
746  
747  
748  
749  
750  
751  
752  
753  
754  
755  
756

## References

1. **Akagawa KS, Komuro I, Kanazawa H, Yamazaki T, Mochida K, and Kishi F.** Functional heterogeneity of colony-stimulating factor-induced human monocyte-derived macrophages. *Respirology (Carlton, Vic)* 11 Suppl: S32-36, 2006.
2. **Alessi DR, Cuenda A, Cohen P, Dudley DT, and Saltiel AR.** PD 098059 is a specific inhibitor of the activation of mitogen-activated protein kinase kinase in vitro and in vivo. *J Biol Chem* 270: 27489-27494, 1995.
3. **Anders S, and Huber W.** Differential expression analysis for sequence count data. *Genome Biol* 11: R106, 2010.
4. **Arredouani M, Yang Z, Ning Y, Qin G, Soininen R, Tryggvason K, and Kobzik L.** The scavenger receptor MARCO is required for lung defense against pneumococcal pneumonia and inhaled particles. *J Exp Med* 200: 267-272, 2004.
5. **Arredouani MS, Palecanda A, Koziel H, Huang YC, Imrich A, Sulahian TH, Ning YY, Yang Z, Pikkarainen T, Sankala M, Vargas SO, Takeya M, Tryggvason K, and Kobzik L.** MARCO is the major binding receptor for unopsonized particles and bacteria on human alveolar macrophages. *J Immunol* 175: 6058-6064, 2005.
6. **Bedoret D, Wallemacq H, Marichal T, Desmet C, Quesada Calvo F, Henry E, Closset R, Dewals B, Thielen C, Gustin P, de Leval L, Van Rooijen N, Le Moine A, Vanderplasschen A, Cataldo D, Drion PV, Moser M, Lekeux P, and Bureau F.** Lung interstitial macrophages alter dendritic cell functions to prevent airway allergy in mice. *J Clin Invest* 119: 3723-3738, 2009.
7. **Bowdish DM, and Gordon S.** Conserved domains of the class A scavenger receptors: evolution and function. *Immunol Rev* 227: 19-31, 2009.
8. **Brydon EW, Smith H, and Sweet C.** Influenza A virus-induced apoptosis in bronchiolar epithelial (NCI-H292) cells limits pro-inflammatory cytokine release. *J Gen Virol* 84: 2389-2400, 2003.
9. **Cai D, Yin S, Yang J, Jiang Q, and Cao W.** Histone deacetylase inhibition activates Nrf2 and protects against osteoarthritis. *Arthritis Res Ther* 17: 269, 2015.
10. **Chen CC, Jeon SM, Bhaskar PT, Nogueira V, Sundararajan D, Tonic I, Park Y, and Hay N.** FoxOs inhibit mTORC1 and activate Akt by inducing the expression of Sestrin3 and Rictor. *Dev Cell* 18: 592-604, 2010.
11. **Dahl M, Bauer AK, Arredouani M, Soininen R, Tryggvason K, Kleeberger SR, and Kobzik L.** Protection against inhaled oxidants through scavenging of oxidized lipids by macrophage receptors MARCO and SR-AI/II. *J Clin Invest* 117: 757-764, 2007.
12. **Damjanovic D, Lai R, Jeyanathan M, Hogaboam CM, and Xing Z.** Marked improvement of severe lung immunopathology by influenza-associated pneumococcal superinfection requires the control of both bacterial replication and host immune responses. *Am J Pathol* 183: 868-880, 2013.
13. **DeLoid GM, Sulahian TH, Imrich A, and Kobzik L.** Heterogeneity in macrophage phagocytosis of *Staphylococcus aureus* strains: high-throughput scanning cytometry-based analysis. *PLoS One* 4: e6209, 2009.
14. **Deng C, Tao R, Yu SZ, and Jin H.** Sulforaphane protects against 6-hydroxydopamine-induced cytotoxicity by increasing expression of heme oxygenase-1 in a PI3K/Akt-dependent manner. *Mol Med Rep* 5: 847-851, 2012.

- 757 15. **Didierlaurent A, Goulding J, Patel S, Snelgrove R, Low L, Bebien M, Lawrence T,**  
758 **van Rijt LS, Lambrecht BN, Sirard JC, and Hussell T.** Sustained desensitization to bacterial  
759 Toll-like receptor ligands after resolution of respiratory influenza infection. *J Exp Med* 205: 323-  
760 329, 2008.
- 761 16. **Divya T, Dineshbabu V, Soumyakrishnan S, Sureshkumar A, and Sudhandiran G.**  
762 Celastrol enhances Nrf2 mediated antioxidant enzymes and exhibits anti-fibrotic effect through  
763 regulation of collagen production against bleomycin-induced pulmonary fibrosis. *Chem Biol*  
764 *Interact* 246: 52-62, 2016.
- 765 17. **Feng J, Meyer CA, Wang Q, Liu JS, Shirley Liu X, and Zhang Y.** GFOLD: a  
766 generalized fold change for ranking differentially expressed genes from RNA-seq data.  
767 *Bioinformatics* 28: 2782-2788, 2012.
- 768 18. **Gaur P, Munjhal A, and Lal SK.** Influenza virus and cell signaling pathways. *Med Sci*  
769 *Monit* 17: Ra148-154, 2011.
- 770 19. **Gay R, Han SN, Marko M, Belisle S, Bronson R, and Meydani SN.** The effect of  
771 vitamin E on secondary bacterial infection after influenza infection in young and old mice. *Ann*  
772 *N Y Acad Sci* 1031: 418-421, 2004.
- 773 20. **Ghoneim HE, Thomas PG, and McCullers JA.** Depletion of alveolar macrophages  
774 during influenza infection facilitates bacterial superinfections. *J Immunol* 191: 1250-1259, 2013.
- 775 21. **Ghosh S, Gregory D, Smith A, and Kobzik L.** MARCO regulates early inflammatory  
776 responses against influenza: a useful macrophage function with adverse outcome. *Am J Respir*  
777 *Cell Mol Biol* 45: 1036-1044, 2011.
- 778 22. **Gonzales XF, Deshmukh A, Pulse M, Johnson K, and Jones HP.** Stress-induced  
779 differences in primary and secondary resistance against bacterial sepsis corresponds with diverse  
780 corticotropin releasing hormone receptor expression by pulmonary CD11c+ MHC II+ and  
781 CD11c- MHC II+ APCs. *Brain Behav Immun* 22: 552-564, 2008.
- 782 23. **Gupta RK, George R, and Nguyen-Van-Tam JS.** Bacterial pneumonia and pandemic  
783 influenza planning. *Emerg Infect Dis* 14: 1187-1192, 2008.
- 784 24. **Han J, Wang M, Jing X, Shi H, Ren M, and Lou H.** (-)-Epigallocatechin gallate  
785 protects against cerebral ischemia-induced oxidative stress via Nrf2/ARE signaling. *Neurochem*  
786 *Res* 39: 1292-1299, 2014.
- 787 25. **Harvey CJ, Thimmulappa RK, Sethi S, Kong X, Yarmus L, Brown RH, Feller-**  
788 **Kopman D, Wise R, and Biswal S.** Targeting Nrf2 signaling improves bacterial clearance by  
789 alveolar macrophages in patients with COPD and in a mouse model. *Sci Transl Med* 3: 78ra32,  
790 2011.
- 791 26. **Hideshima T, Catley L, Yasui H, Ishitsuka K, Raje N, Mitsiades C, Podar K,**  
792 **Munshi NC, Chauhan D, Richardson PG, and Anderson KC.** Perifosine, an oral bioactive  
793 novel alkylphospholipid, inhibits Akt and induces in vitro and in vivo cytotoxicity in human  
794 multiple myeloma cells. *Blood* 107: 4053-4062, 2006.
- 795 27. **Hrincius ER, Liedmann S, Finkelstein D, Vogel P, Gause S, Ehrhardt C,**  
796 **Ludwig S, Hains DS, Webby R, and McCullers JA.** Nonstructural Protein 1 (NS1)-Mediated  
797 Inhibition of c-Abl Results in Acute Lung Injury and Priming for Bacterial Coninfections:  
798 Insights Into 1918 H1N1 Pandemic? *J Infect Dis* 2014.
- 799 28. **Ivanov S, Renneson J, Fontaine J, Barthelemy A, Paget C, Fernandez EM, Blanc F,**  
800 **De Trez C, Van Maele L, Dumoutier L, Huerre MR, Eberl G, Si-Tahar M, Gosset P,**  
801 **Renauld JC, Sirard JC, Faveeuw C, and Trottein F.** Interleukin-22 reduces lung

inflammation during influenza A virus infection and protects against secondary bacterial infection. *J Virol* 87: 6911-6924, 2013.

29. **Jamieson AM, Paskan L, Yu S, Gamradt P, Homer RJ, Decker T, and Medzhitov R.** Role of tissue protection in lethal respiratory viral-bacterial coinfection. *Science* 340: 1230-1234, 2013.

30. **Jo H, Mondal S, Tan D, Nagata E, Takizawa S, Sharma AK, Hou Q, Shanmugasundaram K, Prasad A, Tung JK, Tejada AO, Man H, Rigby AC, and Luo HR.** Small molecule-induced cytosolic activation of protein kinase Akt rescues ischemia-elicited neuronal death. *Proc Natl Acad Sci U S A* 109: 10581-10586, 2012.

31. **Kongchanagul A, Suptawiwat O, Boonarkart C, Kitphati R, Puthavathana P, Uiprasertkul M, and Auewarakul P.** Decreased expression of surfactant protein D mRNA in human lungs in fatal cases of H5N1 avian influenza. *J Med Virol* 83: 1410-1417, 2011.

32. **Kudva A, Scheller EV, Robinson KM, Crowe CR, Choi SM, Slight SR, Khader SA, Dubin PJ, Enelow RI, Kolls JK, and Alcorn JF.** Influenza A inhibits Th17-mediated host defense against bacterial pneumonia in mice. *J Immunol* 186: 1666-1674, 2011.

33. **Kukavica-Ibrulj I, Hamelin ME, Prince GA, Gagnon C, Bergeron Y, Bergeron MG, and Boivin G.** Infection with human metapneumovirus predisposes mice to severe pneumococcal pneumonia. *J Virol* 83: 1341-1349, 2009.

34. **Lagranderie M, Nahori MA, Balazuc AM, Kiefer-Biasizzo H, Lapa e Silva JR, Milon G, Marchal G, and Vargaftig BB.** Dendritic cells recruited to the lung shortly after intranasal delivery of Mycobacterium bovis BCG drive the primary immune response towards a type 1 cytokine production. *Immunology* 108: 352-364, 2003.

35. **Lamb J, Crawford ED, Peck D, Modell JW, Blat IC, Wrobel MJ, Lerner J, Brunet J-P, Subramanian A, Ross KN, Reich M, Hieronymus H, Wei G, Armstrong SA, Haggarty SJ, Clemons PA, Wei R, Carr SA, Lander ES, and Golub TR.** The Connectivity Map: using gene-expression signatures to connect small molecules, genes, and disease. *Science* 313: 1929-1935, 2006.

36. **Langmead B, and Salzberg SL.** Fast gapped-read alignment with Bowtie 2. *Nat Methods* 9: 357-359, 2012.

37. **Lee B, Robinson KM, McHugh KJ, Scheller EV, Mandalapu S, Chen C, Di YP, Clay ME, Enelow RI, Dubin PJ, and Alcorn JF.** Influenza-induced type I interferon enhances susceptibility to gram-negative and gram-positive bacterial pneumonia in mice. *Am J Physiol Lung Cell Mol Physiol* 309: L158-167, 2015.

38. **Lee LN, Dias P, Han D, Yoon S, Shea A, Zakharov V, Parham D, and Sarawar SR.** A mouse model of lethal synergism between influenza virus and Haemophilus influenzae. *Am J Pathol* 176: 800-811, 2010.

39. **Lee YJ, Jeong HY, Kim YB, Lee YJ, Won SY, Shim JH, Cho MK, Nam HS, and Lee SH.** Reactive oxygen species and PI3K/Akt signaling play key roles in the induction of Nrf2-driven heme oxygenase-1 expression in sulforaphane-treated human mesothelioma MSTO-211H cells. *Food Chem Toxicol* 50: 116-123, 2012.

40. **Li N, Ren A, Wang X, Fan X, Zhao Y, Gao GF, Cleary P, and Wang B.** Influenza viral neuraminidase primes bacterial coinfection through TGF-beta-mediated expression of host cell receptors. *Proc Natl Acad Sci U S A* 112: 238-243, 2015.

41. **McAuley JL, Hornung F, Boyd KL, Smith AM, McKeon R, Bennink J, Yewdell JW, and McCullers JA.** Expression of the 1918 influenza A virus PB1-F2 enhances the pathogenesis of viral and secondary bacterial pneumonia. *Cell Host Microbe* 2: 240-249, 2007.

- 848 42. **McCullers JA**. The co-pathogenesis of influenza viruses with bacteria in the lung. *Nat*  
849 *Rev Microbiol* 12: 252-262, 2014.
- 850 43. **McCullers JA**. Effect of antiviral treatment on the outcome of secondary bacterial  
851 pneumonia after influenza. *J Infect Dis* 190: 519-526, 2004.
- 852 44. **McCullers JA, and Bartmess KC**. Role of neuraminidase in lethal synergism between  
853 influenza virus and *Streptococcus pneumoniae*. *J Infect Dis* 187: 1000-1009, 2003.
- 854 45. **McCullers JA, and Rehg JE**. Lethal synergism between influenza virus and  
855 *Streptococcus pneumoniae*: characterization of a mouse model and the role of platelet-activating  
856 factor receptor. *J Infect Dis* 186: 341-350, 2002.
- 857 46. **Medina DL, Fraldi A, Bouche V, Annunziata F, Mansueto G, Spampanato C, Puri**  
858 **C, Pignata A, Martina JA, Sardiello M, Palmieri M, Polishchuk R, Puertollano R, and**  
859 **Ballabio A**. Transcriptional activation of lysosomal exocytosis promotes cellular clearance. *Dev*  
860 *Cell* 21: 421-430, 2011.
- 861 47. **Morimitsu Y, Nakagawa Y, Hayashi K, Fujii H, Kumagai T, Nakamura Y, Osawa**  
862 **T, Horio F, Itoh K, Iida K, Yamamoto M, and Uchida K**. A sulforaphane analogue that  
863 potently activates the Nrf2-dependent detoxification pathway. *J Biol Chem* 277: 3456-3463,  
864 2002.
- 865 48. **Papaiahgari S, Zhang Q, Kleeberger SR, Cho HY, and Reddy SP**. Hyperoxia  
866 stimulates an Nrf2-ARE transcriptional response via ROS-EGFR-PI3K-Akt/ERK MAP kinase  
867 signaling in pulmonary epithelial cells. *Antioxid Redox Signal* 8: 43-52, 2006.
- 868 49. **Pittet LA, Hall-Stoodley L, Rutkowski MR, and Harmsen AG**. Influenza virus  
869 infection decreases tracheal mucociliary velocity and clearance of *Streptococcus pneumoniae*.  
870 *Am J Respir Cell Mol Biol* 42: 450-460, 2010.
- 871 50. **Plotkowski MC, Puchelle E, Beck G, Jacquot J, and Hannoun C**. Adherence of type I  
872 *Streptococcus pneumoniae* to tracheal epithelium of mice infected with influenza A/PR8 virus.  
873 *Am Rev Respir Dis* 134: 1040-1044, 1986.
- 874 51. **Pluddemann A, Mukhopadhyay S, and Gordon S**. The interaction of macrophage  
875 receptors with bacterial ligands. *Expert Rev Mol Med* 8: 1-25, 2006.
- 876 52. **Qi L, Kash JC, Dugan VG, Jagger BW, Lau YF, Sheng ZM, Crouch EC, Hartshorn**  
877 **KL, and Taubenberger JK**. The ability of pandemic influenza virus hemagglutinins to induce  
878 lower respiratory pathology is associated with decreased surfactant protein D binding. *Virology*  
879 412: 426-434, 2011.
- 880 53. **Rehli M, Den Elzen N, Cassady AI, Ostrowski MC, and Hume DA**. Cloning and  
881 characterization of the murine genes for bHLH-ZIP transcription factors TFEC and TFEB reveal  
882 a common gene organization for all MiT subfamily members. *Genomics* 56: 111-120, 1999.
- 883 54. **Rialdi A, Campisi L, Zhao N, Lagda AC, Pietzsch C, Ho JSY, Martinez-Gil L,**  
884 **Fenouil R, Chen X, Edwards M, Metreveli G, Jordan S, Peralta Z, Muñoz-Fontela C,**  
885 **Bouvier N, Merad M, Jin J, Weirauch M, Heinz S, Benner C, van Bakel H, Basler C,**  
886 **García-Sastre A, Bukreyev A, and Marazzi I**. Topoisomerase 1 inhibition suppresses  
887 inflammatory genes and protects from death by inflammation. *Science* 352: aad7993, 2016.
- 888 55. **Robinson KM, Choi SM, McHugh KJ, Mandalapu S, Enelow RI, Kolls JK, and**  
889 **Alcorn JF**. Influenza A exacerbates *Staphylococcus aureus* pneumonia by attenuating IL-1beta  
890 production in mice. *J Immunol* 191: 5153-5159, 2013.
- 891 56. **Robinson KM, Kolls JK, and Alcorn JF**. The immunology of influenza virus-  
892 associated bacterial pneumonia. *Curr Opin Immunol* 34c: 59-67, 2015.

- 893 57. **Robinson KM, Lee B, Scheller EV, Mandalapu S, Enelow RI, Kolls JK, and Alcorn**  
894 **JF.** The role of IL-27 in susceptibility to post-influenza *Staphylococcus aureus* pneumonia.  
895 *Respir Res* 16: 10, 2015.
- 896 58. **Robinson KM, McHugh KJ, Mandalapu S, Clay ME, Lee B, Scheller EV, Enelow**  
897 **RI, Chan YR, Kolls JK, and Alcorn JF.** Influenza A virus exacerbates *Staphylococcus aureus*  
898 pneumonia in mice by attenuating antimicrobial peptide production. *J Infect Dis* 209: 865-875,  
899 2014.
- 900 59. **Roczniak-Ferguson A, Petit CS, Froehlich F, Qian S, Ky J, Angarola B, Walther**  
901 **TC, and Ferguson SM.** The transcription factor TFEB links mTORC1 signaling to  
902 transcriptional control of lysosome homeostasis. *Sci Signal* 5: ra42, 2012.
- 903 60. **Rothberg MB, Haessler SD, and Brown RB.** Complications of viral influenza. *Am J*  
904 *Med* 121: 258-264, 2008.
- 905 61. **Sardiello M, Palmieri M, di Ronza A, Medina DL, Valenza M, Gennarino VA, Di**  
906 **Malta C, Donaudy F, Embrione V, Polishchuk RS, Banfi S, Parenti G, Cattaneo E, and**  
907 **Ballabio A.** A gene network regulating lysosomal biogenesis and function. *Science* 325: 473-  
908 477, 2009.
- 909 62. **Schneider C, Nobs SP, Heer AK, Kurrer M, Klinke G, van Rooijen N, Vogel J, and**  
910 **Kopf M.** Alveolar macrophages are essential for protection from respiratory failure and  
911 associated morbidity following influenza virus infection. *PLoS Pathog* 10: e1004053, 2014.
- 912 63. **Settembre C, Di Malta C, Polito VA, Garcia Arencibia M, Vetrini F, Erdin S, Erdin**  
913 **SU, Huynh T, Medina D, Colella P, Sardiello M, Rubinsztein DC, and Ballabio A.** TFEB  
914 links autophagy to lysosomal biogenesis. *Science* 332: 1429-1433, 2011.
- 915 64. **Settembre C, Zoncu R, Medina DL, Vetrini F, Erdin S, Erdin S, Huynh T, Ferron**  
916 **M, Karsenty G, Vellard MC, Facchinetti V, Sabatini DM, and Ballabio A.** A lysosome-to-  
917 nucleus signalling mechanism senses and regulates the lysosome via mTOR and TFEB. *Embo j*  
918 31: 1095-1108, 2012.
- 919 65. **Shahangian A, Chow EK, Tian X, Kang JR, Ghaffari A, Liu SY, Belperio JA,**  
920 **Cheng G, and Deng JC.** Type I IFNs mediate development of postinfluenza bacterial  
921 pneumonia in mice. *J Clin Invest* 119: 1910-1920, 2009.
- 922 66. **Siegel SJ, Roche AM, and Weiser JN.** Influenza promotes pneumococcal growth during  
923 coinfection by providing host sialylated substrates as a nutrient source. *Cell Host Microbe* 16:  
924 55-67, 2014.
- 925 67. **Smith MW, Schmidt JE, Rehg JE, Orihuela CJ, and McCullers JA.** Induction of pro-  
926 and anti-inflammatory molecules in a mouse model of pneumococcal pneumonia after influenza.  
927 *Comp Med* 57: 82-89, 2007.
- 928 68. **Stegemann S, Dahlberg S, Kroger A, Gereke M, Bruder D, Henriques-Normark B,**  
929 **and Gunzer M.** Increased susceptibility for superinfection with *Streptococcus pneumoniae*  
930 during influenza virus infection is not caused by TLR7-mediated lymphopenia. *PLoS One* 4:  
931 e4840, 2009.
- 932 69. **Steingrimsson E, Tessarollo L, Reid SW, Jenkins NA, and Copeland NG.** The bHLH-  
933 Zip transcription factor Tfeb is essential for placental vascularization. *Development* 125: 4607-  
934 4616, 1998.
- 935 70. **Subramaniam R, Barnes PF, Fletcher K, Boggaram V, Hillberry Z,**  
936 **Neuenschwander P, and Shams H.** Protecting against post-influenza bacterial pneumonia by  
937 increasing phagocyte recruitment and ROS production. *J Infect Dis* 209: 1827-1836, 2014.

- 938 71. **Sulahian TH, Imrich A, Deloid G, Winkler AR, and Kobzik L.** Signaling pathways  
939 required for macrophage scavenger receptor-mediated phagocytosis: analysis by scanning  
940 cytometry. *Respir Res* 9: 59, 2008.
- 941 72. **Sun K, and Metzger DW.** Influenza infection suppresses NADPH oxidase-dependent  
942 phagocytic bacterial clearance and enhances susceptibility to secondary methicillin-resistant  
943 *Staphylococcus aureus* infection. *J Immunol* 192: 3301-3307, 2014.
- 944 73. **Sun K, and Metzger DW.** Inhibition of pulmonary antibacterial defense by interferon-  
945 gamma during recovery from influenza infection. *Nat Med* 14: 558-564, 2008.
- 946 74. **Sun SY.** Enhancing perifosine's anticancer efficacy by preventing autophagy. *Autophagy*  
947 6: 184-185, 2010.
- 948 75. **Tapia E, Garcia-Arroyo F, Silverio O, Rodriguez-Alcocer AN, Jimenez-Flores AB,**  
949 **Cristobal M, Arellano AS, Soto V, Osorio-Alonso H, Molina-Jijon E, Pedraza-Chaverri J,**  
950 **and Sanchez-Lozada LG.** Mycophenolate mofetil and curcumin provide comparable  
951 therapeutic benefit in experimental chronic kidney disease: role of Nrf2-Keap1 and renal  
952 dopamine pathways. *Free Radic Res* 50: 781-792, 2016.
- 953 76. **Thakur SA, Beamer CA, Migliaccio CT, and Holian A.** Critical role of MARCO in  
954 crystalline silica-induced pulmonary inflammation. *Toxicol Sci* 108: 462-471, 2009.
- 955 77. **Thimmulappa RK, Mai KH, Srisuma S, Kensler TW, Yamamoto M, and Biswal S.**  
956 Identification of Nrf2-regulated genes induced by the chemopreventive agent sulforaphane by  
957 oligonucleotide microarray. *Cancer Res* 62: 5196-5203, 2002.
- 958 78. **Tiller GR, and Garsin DA.** Of worms and men: HLH-30 and TFEB regulate tolerance  
959 to infection. *Immunity* 40: 857-858, 2014.
- 960 79. **van der Sluijs KF, Nijhuis M, Levels JH, Florquin S, Mellor AL, Jansen HM, van**  
961 **der Poll T, and Lutter R.** Influenza-induced expression of indoleamine 2,3-dioxygenase  
962 enhances interleukin-10 production and bacterial outgrowth during secondary pneumococcal  
963 pneumonia. *J Infect Dis* 193: 214-222, 2006.
- 964 80. **van der Sluijs KF, van der Poll T, Lutter R, Juffermans NP, and Schultz MJ.** Bench-  
965 to-bedside review: bacterial pneumonia with influenza - pathogenesis and clinical implications.  
966 *Crit Care* 14: 219, 2010.
- 967 81. **van der Sluijs KF, van Elden LJ, Nijhuis M, Schuurman R, Florquin S, Shimizu T,**  
968 **Ishii S, Jansen HM, Lutter R, and van der Poll T.** Involvement of the platelet-activating factor  
969 receptor in host defense against *Streptococcus pneumoniae* during postinfluenza pneumonia. *Am*  
970 *J Physiol Lung Cell Mol Physiol* 290: L194-199, 2006.
- 971 82. **van der Sluijs KF, van Elden LJ, Nijhuis M, Schuurman R, Pater JM, Florquin S,**  
972 **Goldman M, Jansen HM, Lutter R, and van der Poll T.** IL-10 is an important mediator of the  
973 enhanced susceptibility to pneumococcal pneumonia after influenza infection. *J Immunol* 172:  
974 7603-7609, 2004.
- 975 83. **Visvikis O, Ihuegbu N, Labed SA, Luhachack LG, Alves AM, Wollenberg AC,**  
976 **Stuart LM, Stormo GD, and Irazoqui JE.** Innate host defense requires TFEB-mediated  
977 transcription of cytoprotective and antimicrobial genes. *Immunity* 40: 896-909, 2014.
- 978 84. **Vomhof-Dekrey EE, and Picklo MJ, Sr.** The Nrf2-antioxidant response element  
979 pathway: a target for regulating energy metabolism. *J Nutr Biochem* 23: 1201-1206, 2012.
- 980 85. **Wang C, Armstrong SM, Sugiyama MG, Tabuchi A, Krauszman A, Kuebler WM,**  
981 **Mullen B, Advani S, Advani A, and Lee WL.** Influenza Primes Human Lung Microvascular  
982 Endothelium to Leak upon Exposure to *Staphylococcus aureus*. *Am J Respir Cell Mol Biol* 2015.

- 983 86. **Wang Y, Wang B, Du F, Su X, Sun G, Zhou G, Bian X, and Liu N.** Epigallocatechin-  
984 3-Gallate Attenuates Oxidative Stress and Inflammation in Obstructive Nephropathy via NF-  
985 kappaB and Nrf2/HO-1 Signalling Pathway Regulation. *Basic Clin Pharmacol Toxicol* 2015.
- 986 87. **Wang Z, Zhou S, Sun C, Lei T, Peng J, Li W, Ding P, Lu J, and Zhao Y.** Interferon-  
987 gamma Inhibits Nonopsonized Phagocytosis of Macrophages via an mTORC1-c/EBPbeta  
988 Pathway. *J Innate Immun* 2014.
- 989 88. **Winkler AR, Nocka KH, Sulahian TH, Kobzik L, and Williams CM.** In vitro  
990 modeling of human alveolar macrophage smoke exposure: enhanced inflammation and impaired  
991 function. *Experimental lung research* 34: 599-629, 2008.
- 992 89. **Yang Z, Chiou TT-Y, Stossel TP, and Kobzik L.** Plasma gelsolin improves lung host  
993 defense against pneumonia by enhancing macrophage NOS3 function. *Am J Physiol Lung Cell*  
994 *Mol Physiol* 309: L11-16, 2015.
- 995 90. **Yu H, Shi L, Zhao S, Sun Y, Gao Y, Sun Y, and Qi G.** Triptolide Attenuates  
996 Myocardial Ischemia/Reperfusion Injuries in Rats by Inducing the Activation of Nrf2/HO-1  
997 Defense Pathway. *Cardiovasc Toxicol* 16: 325-335, 2016.
- 998 91. **Zavitz CC, Bauer CM, Gaschler GJ, Fraser KM, Strieter RM, Hogaboam CM, and**  
999 **Stampfli MR.** Dysregulated macrophage-inflammatory protein-2 expression drives illness in  
1000 bacterial superinfection of influenza. *J Immunol* 184: 2001-2013, 2010.
- 1001

Figure 1

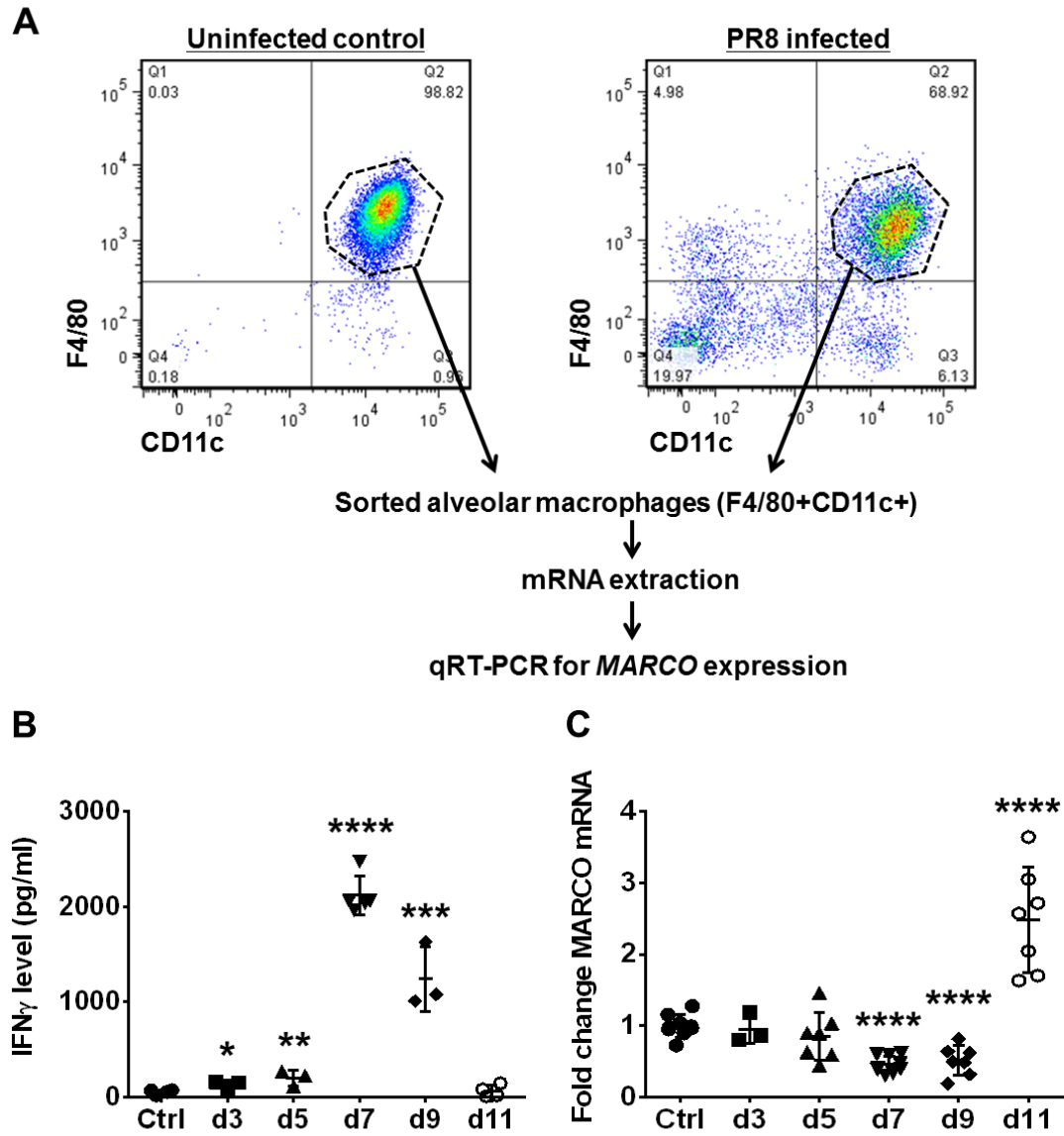


**Figure 2**

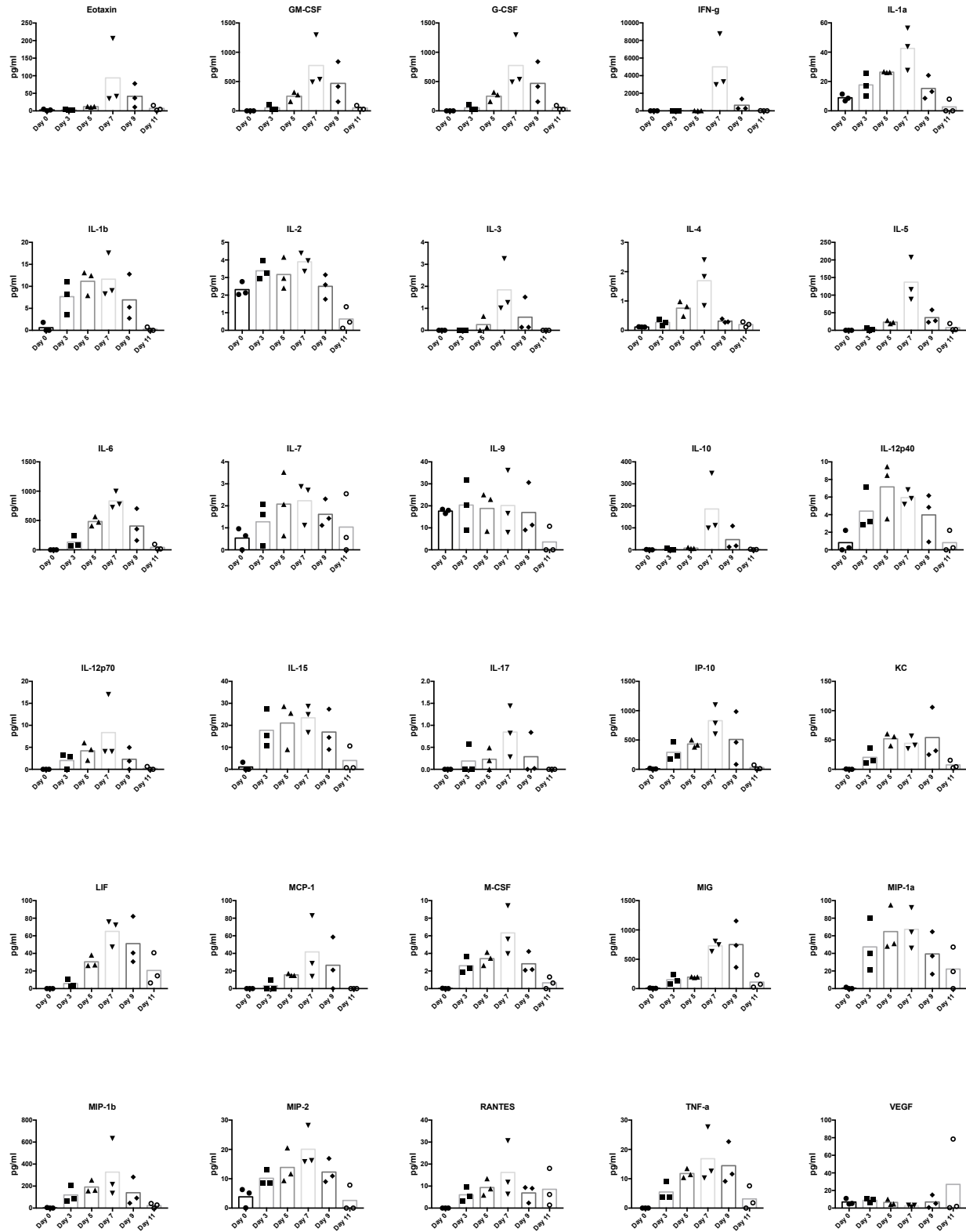


**Figure 3**

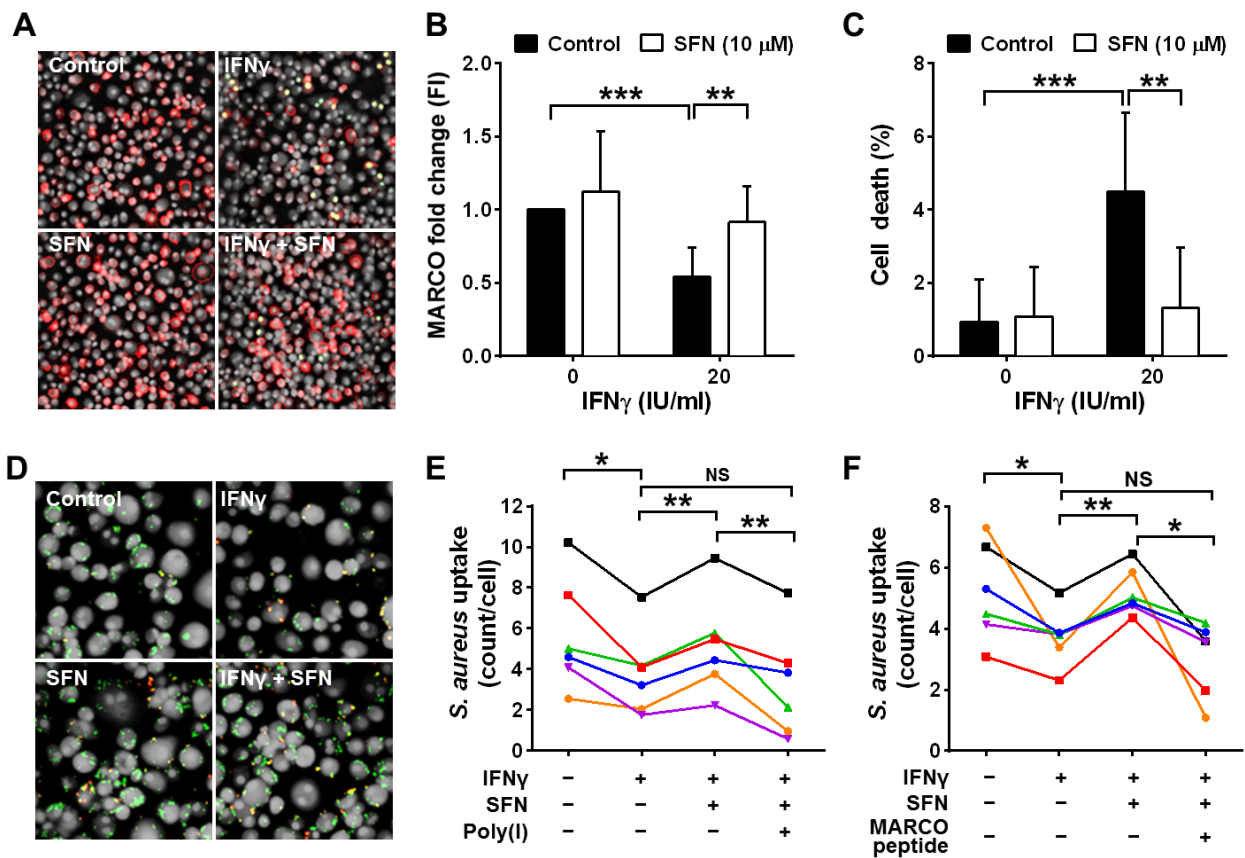


Figure 4

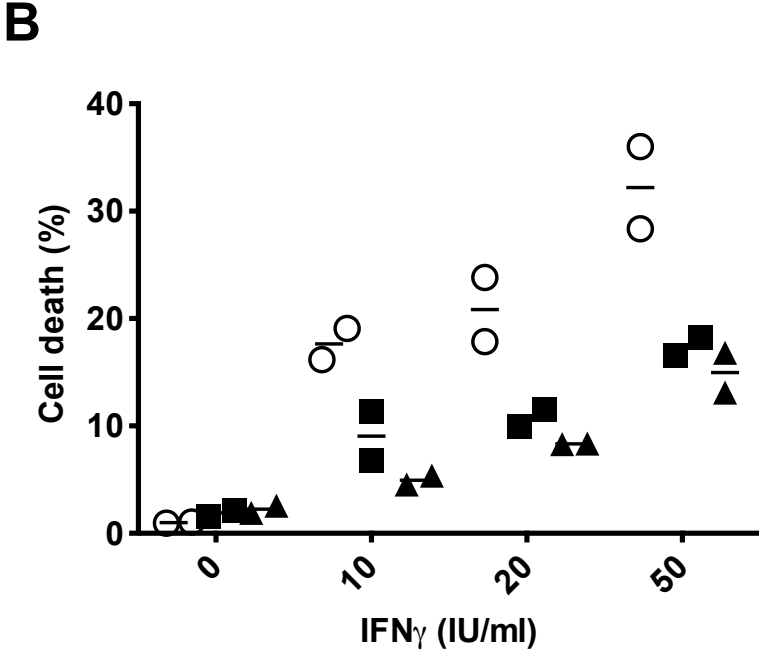
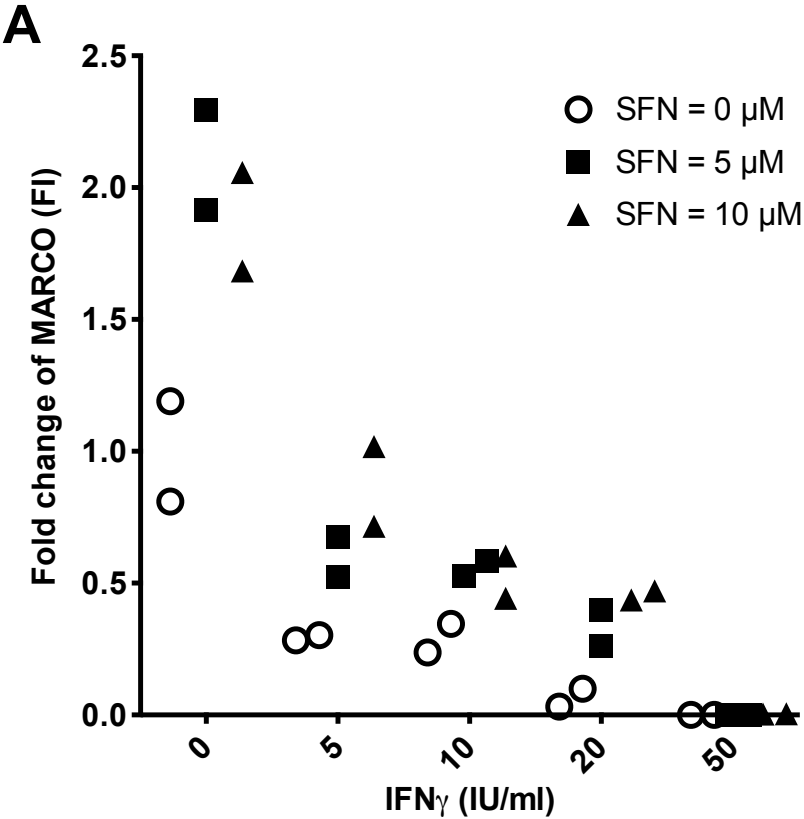


Figure 5

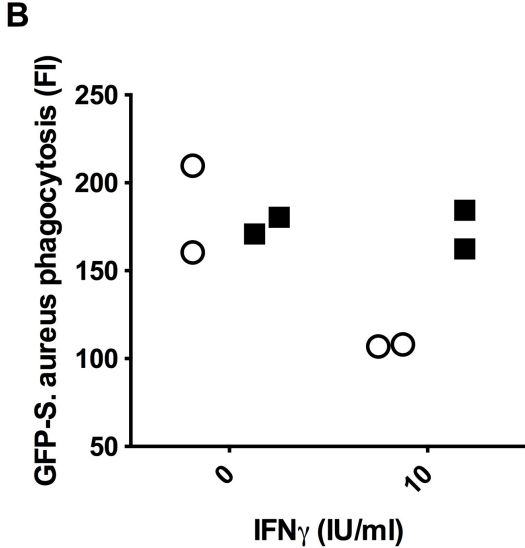
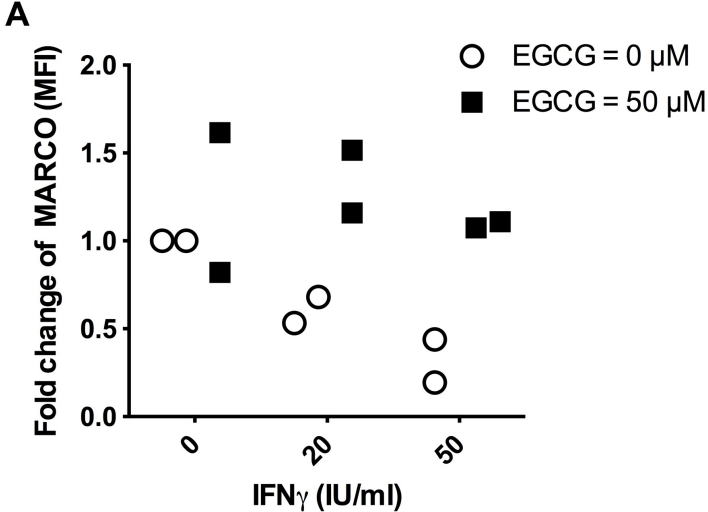


Figure 6

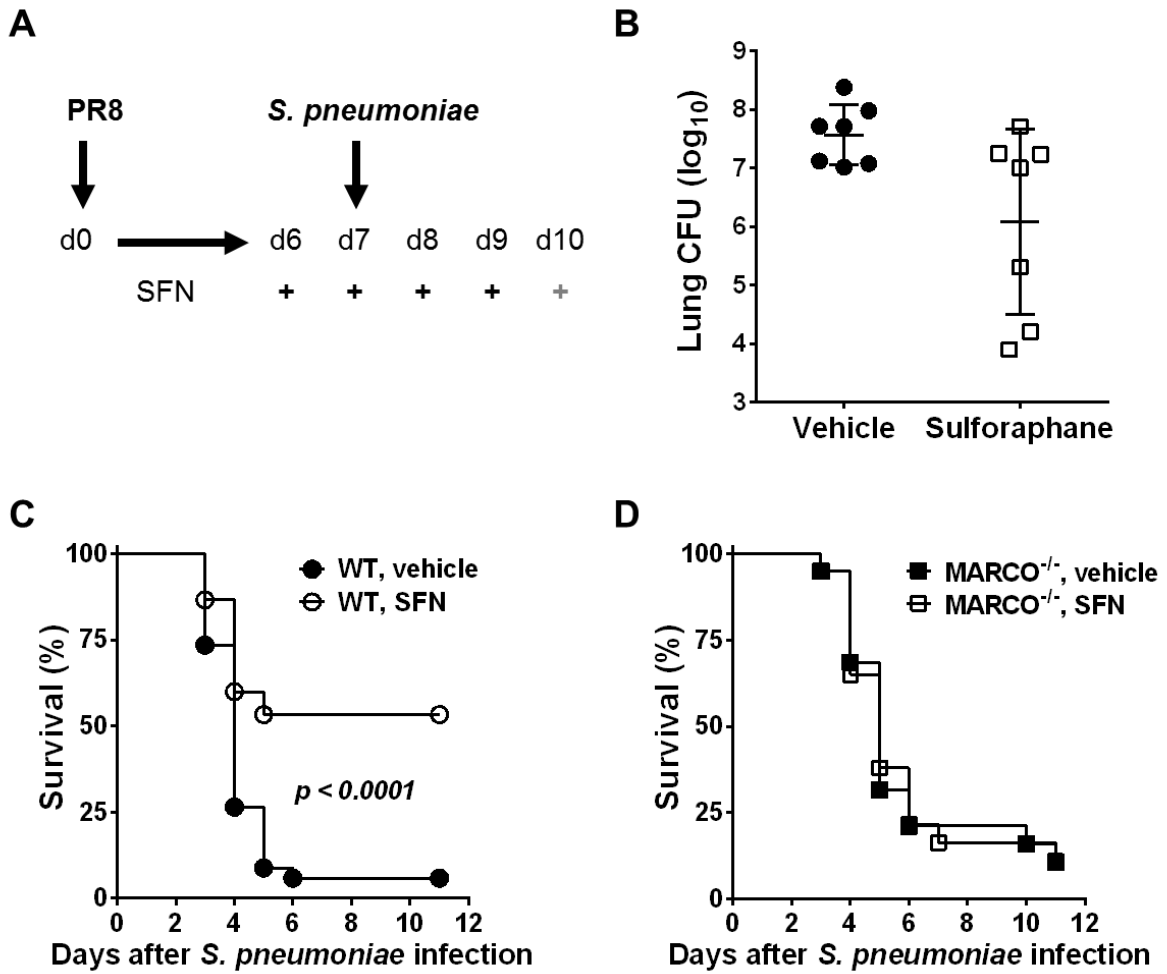
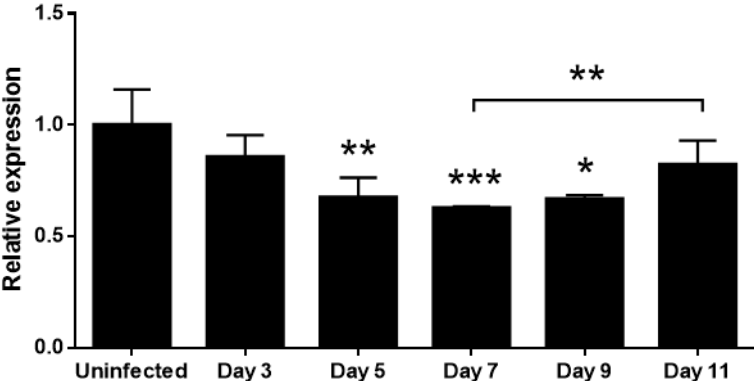


Figure 7

A



B

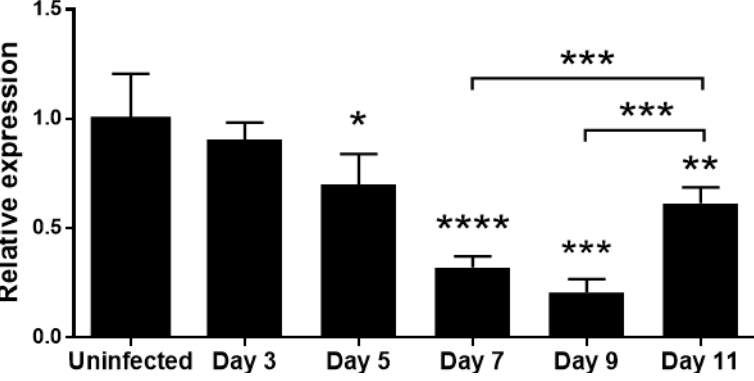
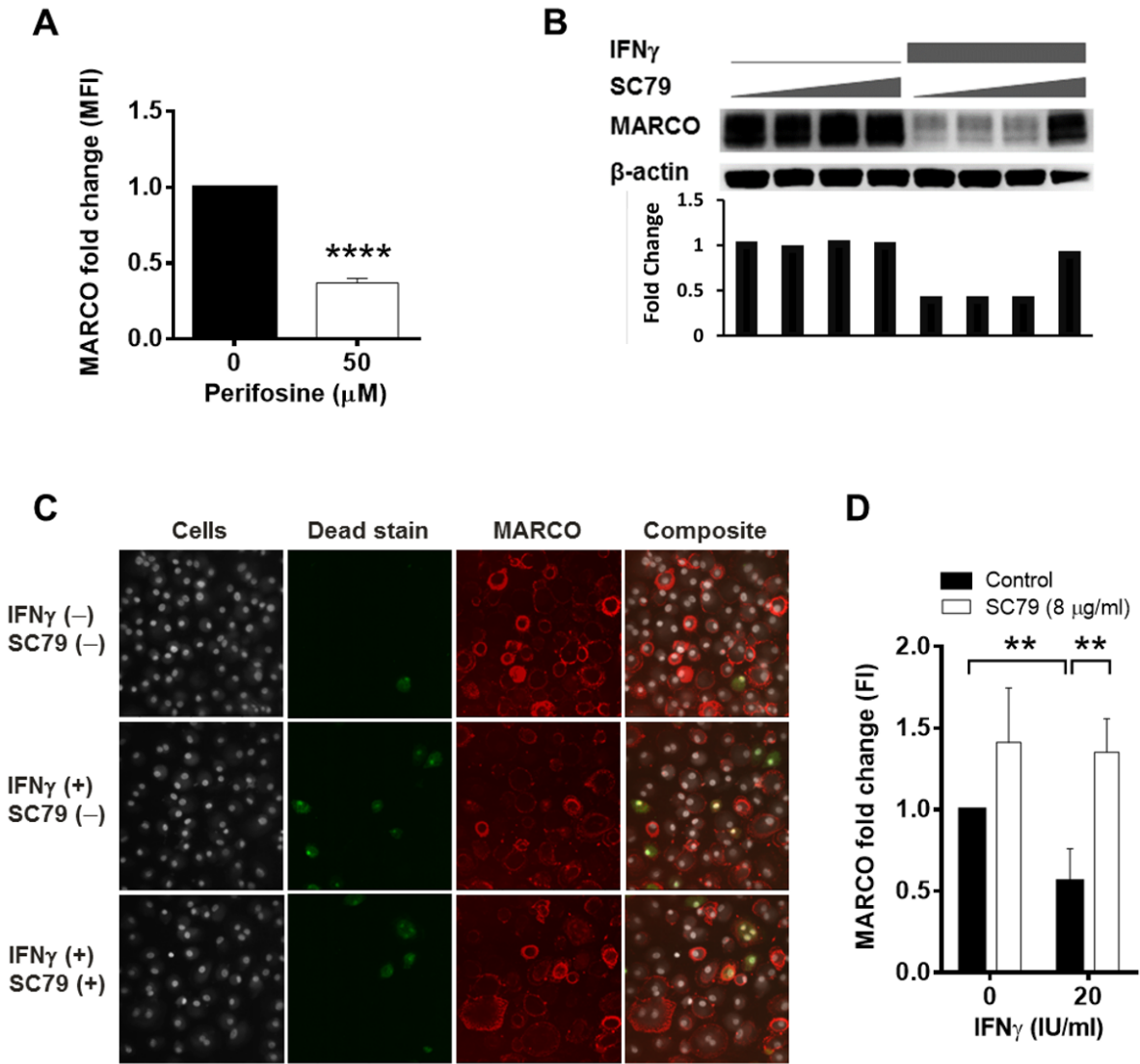


Figure 8



**Figure 9**

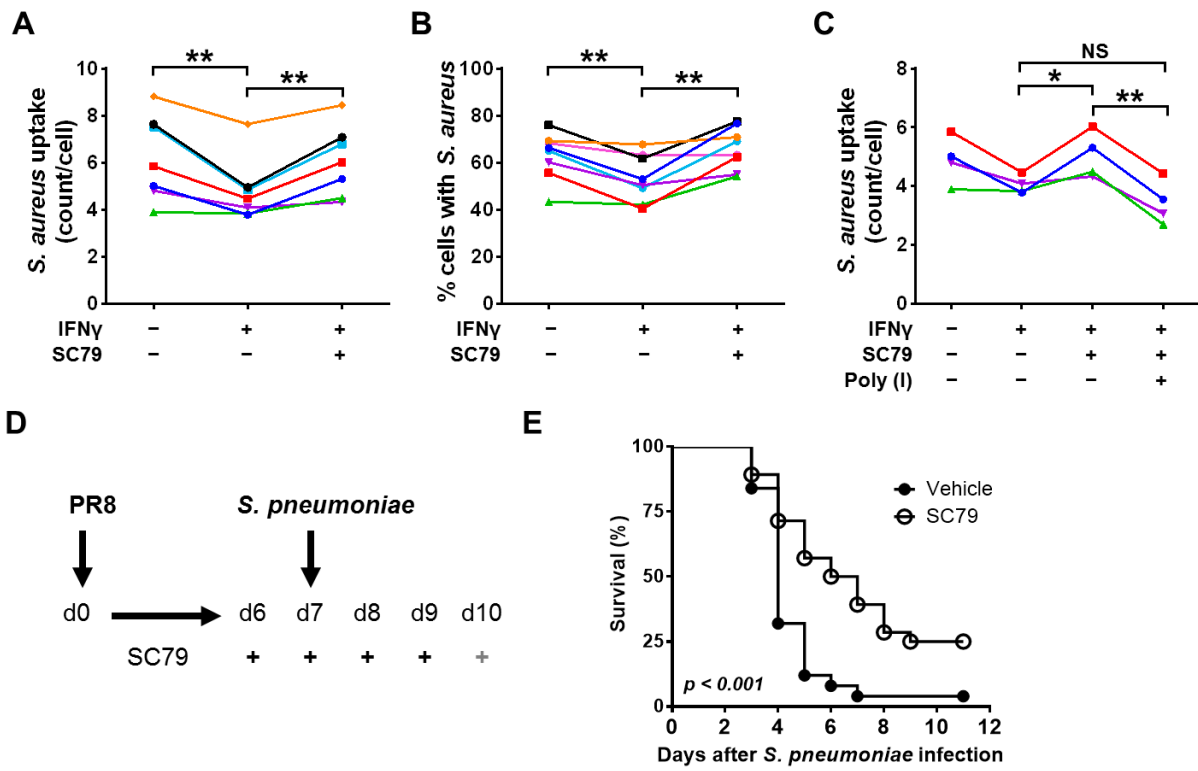
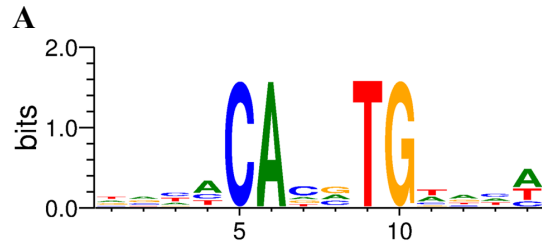


Figure 10



**B**

CTCTGGTCTCTAGCCAGAGGTGAAGTGACTA **CACTTG**ACATCCACTAAGTGCTTCCTTTAAGAACAGG  
GATCCTCAATAATTAGCCCATGACATTTTCTAATAAGTCCCCTCCCACACCCATGAGAATCAAAGATG  
AGCTGACCAGGCAGAGGCAGAGGGAGAGCAGGGAGCTCTGCCAGGCTAAGTGAGCGGGTTCCTTTGC  
CTAGGGGACTGCCCTCCAGTGGGCAAATCCCCTGTGTCTCAATTATCTGGTCTGTCTACCCCCAGA  
CTCTAGCTGGAGCCATCACTTCCTCATTTCOAATTTTCTCTTTAAATTTTTCTGTCTGGCTTCTGTCTG  
TTGTCTCTGGCGGAACCAGTGACTTCCTGAATGTTGAAATTGTGGGCGCCACGGGGGACCTCTGCTTT  
TCAGGGCACTGCTAGGAGCTCACTTCCTGAGTTTCATCCCCTTCACTTTCTGACATAACCACGGGCCA  
AAGAAAGTGACTTCGCCTGGCACAGCTTCACTTCCTGC **CACCTG**TCTTCCTCACCTTTACATTTCAA  
TAGGCCAAAAGTCTACGGCTCCCCTGCTCCAGGCTGTCCCACCTCTGAGAGGCTG **CACCTG**CCCTCCTT  
CCTCCCTGGAGGGCCTTTGCCTCATCTTGATCTGGATCAATCCCCATTATCCTTTAAGCCCAGCTCTG  
GTATCTGATATCTCTTGATT **CAGATG**ATAAAGCTATTTGTCAATTTCTGCCCTGTCTCCCCTGCCTCCC  
GGCACTTCTGTCTTTTCAGGGACATCAACCTTTGCCGCACTTCACAGCAATTTTCTGGAATGTAGTTGT  
AGCCGCAACCATCTTGCAATGGTAGACTGTGAATATCTTTCAAGAAAAAGGCCATTTCTTCATCTCCTC  
GGTGCCCAGCAGGCTCACAATGTCTCTAATGATAATAACAACAACATGACCATAGTGTATTACCTA  
ATACTTCCATCCTAGCCACCTTATATGATTTAATTCATTTAAGGCTCACGAAATTCATATCTTCCTTATT  
TATACAAACAGAAGAGTGAGATGCTCAAAGCT **CAAGTG**ATTTGCCTACTGCCAGACAGCCCCTATGTG  
GAAGAGGTGGAATTTGAAGCCAGGCATTCTAGCTCTTAGTGTCTGTGTCTTAACCACCATGCTATACA  
GCAT **CCCTGGTAGAGATGCCTGAC**GGGAGGGAGAGAGGGGAGAAGCTACTTTCTTAAGGAGCTCAG  
ATCTCACTGGGCCTGGACAAGGA **CACCTG**TAA **CACATG**TA **CACATGTG**CA **CACATGTG**TACACACAC  
AGAGAGAGAACATGGGAAAACACTACAAGAAGAAATACTAAGTGCTAAAATGT **GTGGTTCAGAGCAAGG**  
**CTTC**TCAAACCTGTAATGTGTATATAAAT **CACCTG**GGGATCTAGTTAAACTGTAGATTTGGATTTGATCT  
GATGGGGTGGGACCAGAGACTCATTGTTAGAA **CAAGTG**AACTTGCATTTCTAACAAGTTCT **CAGGTG**A  
TACTAATACTGCTGGTCCATGGACCACACTTTGAGCAGCAAGGATGAACTCTAAAGGTTGAGGCAGGT  
CAGAGAAGGGAGATTTCACTGTGGGCTGGAGAGGCTCTGGGACAGAGAGCTGAGTCTGGGCCATGG  
CAGGGCTTGGTTGGCCCTCTCTGGAGCCATCCAGCTTTTGGGTCTCAGGGACCTGGGAGTGACGGGTG  
CATTCAAGAGGCCCGTAACTTGTGTCCCAAAGCCTCCTCGATCCCCCTTAAACAAGCAGCAGCACTGTGT  
GGGAGATC **CACATGTG**AATAGCCCGTGTGTTGAGAAATGTCCAATCCTGATCATGTCAGGAAACATCCT  
GCAAATCTGAAATCAGAGCCAAAGGGAAGTGCTGCGAGGTTTACAAC **CAGCTG**CAGTGGTTTCGATG  
GGAAGGATCTTTCTC **CAAGTG**GTTCTCTTGAGGGGAGCATTCTGTCTGGCTCCAGGACTTTGGCCATC  
TATAAAGCTTGGCAATGAGAAATAAGAAAATTCTCAAGGAGGACGAGCTCTTGAGTGAGACCCAACA  
AGCTGCTTTTACCAAATTGCAATGGAGCCTTTCGAAATCAATGGATGAGGAGTGTAATTTTCACT  
GTACCCTCTAGAAGCACAGTGCAACTTGCATCCCTCTTCTGCCATCACCTCCAGCCTCCCTCATTAG  
ACAAGCCTC

**Figure 11**

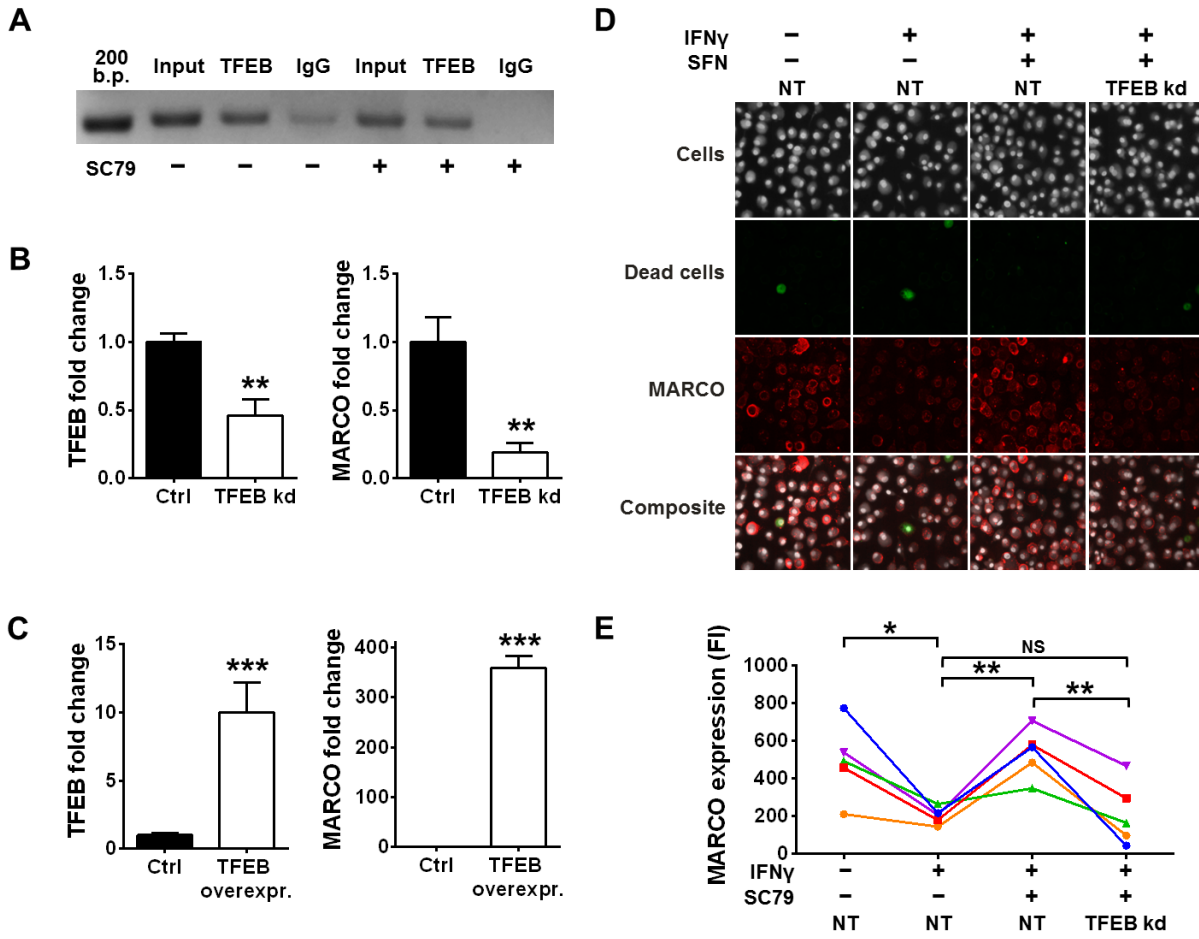


Figure 12

